1242

TRANSPORTATION RESEARCH RECORD

Innovative Earth-Retaining Systems

TRANSPORTATION RESEARCH BOARD
NATIONAL RESEARCH COUNCIL
WASHINGTON, D.C. 1989

Transportation Research Record 1242
Price: $9.00

mode
1 highway transportation

subject areas
25 structures design and performance
33 construction
62 soil foundations
63 soil and rock mechanics

Printed in the United States of America

Library of Congress Cataloging-in-Publication Data
National Research Council. Transportation Research Board.

Innovative earth retaining systems.
p. cm—(Transportation research record, ISSN 0361-1981 ; 1242)
Contents: Overview of Pennsylvania generic design and construction specifications for proprietary (prefabricated) walls/by M. G. Patel . . . and others—Evaluation of earth pressures acting on slide suppressor walls/by S. G. Wright, W. M. Isenhower, M. K. Kayyal—Design procedures for slide suppressor walls/by W. M. Isenhower, S. G. Wright, and M. K. Kayyal—Ter-voile retaining works/Valerian Curt—Dynamic stability of soil reinforced walls/by John Vrymoed—Performance of a 62-foot high soil reinforced wall in California's North Coast range/by Kenneth A. Jackura.
ISBN 0-309-04959-8
1. Retaining walls—Design and construction. I. Series.
TE7.H5 no. 1242
[TA770]
388 s—dc20
[625.7'3] 90-34797
CIP

Sponsorship of Transportation Research Record 1242

GROUP 2—DESIGN AND CONSTRUCTION OF TRANSPORTATION FACILITIES
Chairman: Raymond A. Forsyth, California Department of Transportation

Soil Mechanics Section
Chairman: Michael G. Katona, TRW

Committee on Foundations of Bridges and Other Structures
Chairman: Richard S. Cheney, Federal Highway Administration, U.S. Department of Transportation
Secretary: Richard P. Long, University of Connecticut
Francois J. Baguelin, Jean-Louis Briaud, Bernard E. Butler, Murty S. Devata, Albert F. DiMillio, Victor Elias, Richard L. Engel, Bengt H. Fellenius, George G. Goble, Richard J. Goettle III, James S. Graham, Robert C. Houghton, Alan P. Kilian, Hugh S. Lacy, Robert M. Leary, John F. Ledbetter, Jr., Larry Lockett, Randolph W. Losch, Lyle K. Moulton, Peter J. Nicholson, Michael Wayne O'Neill, Harvey E. Wahls, John L. Walkinshaw, Gdalyah Wiseman

G. P. Jayaprakash, Transportation Research Board staff

The organizational units, officers, and members are as of December 31, 1988.

Transportation Research Board publications are available by ordering directly from TRB. They may also be obtained on a regular basis through organizational or individual affiliation with TRB; affiliates or library subscribers are eligible for substantial discounts. For further information, write to the Transportation Research Board, National Research Council, 2101 Constitution Avenue, N.W., Washington, D.C. 20418.

Transportation Research Record 1242

Contents

Foreword

This Record contains six papers that are of interest to engineers who design, construct, and monitor performance of earth-retaining structures.

Although for the past 20 years proprietary earth-retaining walls have been constructed in the United States, no generic design or construction specifications are available in the nation. Patel, Shah, Dash, and Ved present a generic specification developed in Pennsylvania for prefabricated walls. They give an overview of the policy and procedure, design, and construction requirements of mechanically stabilized earth and modular walls.

The next two papers, by Wright, Isenhower, and Kayyal, describe results of research conducted in Texas on slide suppressor walls. The first paper presents procedures for calculating forces on the walls using shear strength parameters that are back-calculated from the slide information. The second paper gives information on design procedures for slide suppressor walls.

Curt presents information on the design and construction of a proprietary retaining wall. The wall consists of a U-shaped cell made of corrugated steel sheet or mesh that retains the backfill material. According to the author, interaction between the mass to be retained and the structural element provides the stability to the structure.

The last two papers in this Record concern a 62-foot-high soil-retaining wall constructed in California. The paper by Vrymoed describes a method developed to determine the static and dynamic stability of that wall. Jackura reports on the results of instrumentation used for the monitoring of construction and analysis of the long-term stability of the wall. He indicates that, 8 months after construction, all observed stresses and movements were within the acceptable limits.

Overview of Pennsylvania's Generic Design and Construction Specifications for Prefabricated Walls

M. G. PATEL, R. N. SHAH, U. DASH, AND N. V. VED

The introduction of proprietary walls in the early 1970s has necessitated the development of generic specifications to encourage competition. The Pennsylvania Department of Transportation (PennDOT) has developed such specifications to combine the mechanically stabilized earth wall with the modular wall. This combination creates a prefabricated wall. This paper gives an overview of the policy and procedure, design, and construction requirements for prefabricated walls. PennDOT uses prefabricated walls as an alternative to conventional reinforced-concrete walls. The discussion covers applicability of these walls to specific site and loading conditions, limitations, tolerances, factors of safety, dimensional limitations, design parameters, drainage, and life requirements. The special design and loading considerations are also presented.

In the early 1970s proprietary walls were introduced in the United States and over 40 proprietary walls have since been constructed or are under construction in Pennsylvania. However, no generic design or construction specifications are available nationally. The design and construction specifications developed by the proprietary wall suppliers have been used, with a few modifications, by the Pennsylvania Department of Transportation (PennDOT). It is believed that the rest of the country also uses the suppliers' design and construction specifications, as this field has evolved rapidly during the last decade.

Because of the impending expiration of most patents to proprietary walls and their frequent use in Pennsylvania, PennDOT developed generic design and construction specifications for the mechanically stabilized earth (MSE) wall and the modular (gravity type) wall. When these walls are combined, a prefabricated wall is created. (In 1985, PennDOT retained a consultant and undertook this project in order to update all sections of *Design Manual, Part 4* (*1*) and to use the latest advancements in the bridge design technology.)

The development of these specifications was important because PennDOT permits alternative designs by contractors in the construction stage of highway and bridge projects. These generic design specifications and a general outline plan provide a common base for preliminary design to determine bid quantities by contractors during the bidding stage.

This paper is a condensed version of the Prefabricated Walls Section of the PennDOT *Design Manual, Part 4* (DM-4) (*1*). The DM-4 may be used for specific references and detailed commentary on the specifications.

An overview of the policy, procedure, and design requirements for MSE and modular walls is given. The design criteria include structure selection (e.g., technical considerations and restrictions, foundation submissions, permitted settlement), design parameters (e.g., structure dimensions, earth pressures, external and internal stability, bearing capacity and foundation stability, pullout design parameters, allowable stresses, factors of safety, drainage requirements, design life requirements), and special design considerations. The specifications for material and construction of these walls, including specific requirements of special fill material for drainability and friction, are available from PennDOT.

This paper also gives an overview of how these specifications are implemented in an open alternative bidding environment. It should be noted that bidders are not required to identify chosen wall type until after the bids have been accepted. PennDOT has been permitting alternative designs by contractors since the early 1980s. Because prefabricated walls have been noticeably economical when marginal sites with poor-to-moderate foundation soils are used and also when the total area is greater than 2,000 ft^2, PennDOT has been permitting their usage even for abutments. Alternative designs by contractor concept or value engineering concept are acceptable.

OVERVIEW OF POLICY AND PROCEDURE

General

Approved prefabricated walls are permitted in competition with conventional reinforced-concrete walls where conventional wall design is provided. If conventional walls are clearly not competitive, they should not be designed.

During the design phase of a project, if it becomes necessary for the designer to obtain detailed information on any of the approved prefabricated-wall companies, the suppliers of all wall types should be contacted to offer the same degree of involvement. (As of November 1988 PennDOT approved reinforced earth, retained earth, and Doublewal® prefabricated walls.)

Pennsylvania Department of Transportation, Transportation and Safety Building, Harrisburg, Pa. 17120.

Systems Approval

All new wall systems should go through PennDOT's product evaluation or experimental item approval process, or both, prior to their unrestricted usage on PennDOT projects.

Selection Procedure

All feasible, innovative, cost-saving alternatives should be considered, as follows:

- All approved and feasible wall systems should be used for a project,
- Value engineering: contractors may propose any cost-saving, equivalent approved alternative, and
- Experimental systems will not be permitted as alternatives.

Economic Considerations for Project Selection

A prefabicated retaining wall for a particular project requires the determination of its technical feasibility and its comparative economy.

MSE walls are generally more economical than conventional walls when

- The retaining wall has a total area greater than 2,000 ft^2,
- The average wall height is greater than 10 ft with no traffic barrier,
- The average wall height is greater than 15 ft with a traffic barrier, or
- A conventional wall requires a deep foundation and the anticipated settlements of MSE walls are tolerable.

Concrete modular systems are generally more economical when

- The walls are to be constructed in cut situations,
- The average wall height is greater than 8 ft, or
- The wall area is greater than 500 ft^2.

Specific project conditions, as outlined below, may reduce the cost-effectiveness of prefabricated wall systems:

- Availability and high cost of selected backfill,
- Alignment complications requiring many turning points and highly irregular finished grades, and
- Necessity for temporary excavation support systems during construction.

Plan Preparation

When prefabricated walls are permitted as an alternative, the following minimum information should be contained in the bid plans:

- Wall geometry information (alignment, length, profile, elevation, ground profile, cross section showing excavation and backfill, right-of-way limits, high water elevation, and scour protection),
- Wall appurtenance information (traffic barriers, copings, drainage, lighting, utilities, and architectural treatment if warranted),
- Construction sequence requirements (stage construction, traffic controls, and construction specifications),
- Design information (bearing capacity of substrata; external loads due to bridge, sign, or lighting structures; anticipated settlement; and allowable deviations),
- Foundation information (drained angle of internal friction, undrained shear strength and density of the substrata materials, boring logs, and water table), and
- Random backfill information (drained angle of internal friction, cohesive strength, and density).

Also included in the bid plans should be bid quantities and special instructions, and the understanding that the designer will check external stability (overturning, sliding, settlement, overall slope stability, and bearing pressures) based upon estimated base width of 0.7 of the height.

Requirements for Contractor Prepared Plans

The successful bidder should prepare a detailed design and drawings for the wall type selected. The design should include the following minimum requirements:

- Internal and external stability must meet the design parameters outlined in the next section.
- Detailed drawings must show all the data mentioned earlier under Plan Preparation and the information needed to prepare the shop drawings and construct the wall. PennDOT's drafting and detailing standards must be followed (*1*). The design must be developed by a professional engineer registered in Pennsylvania.
- Shop drawing preparation and the submittal requirements must follow PennDOT practices.

OVERVIEW OF DESIGN SPECIFICATIONS

General and Primary Systems

MSE walls

MSE walls, some of which are proprietary, employ either strip or grid-type, metallic, inextensible tensile reinforcements in the soil mass and a discrete modular precast concrete facing, which is vertical or near vertical.

Concrete Modular Systems

Concrete modular systems, some of which are proprietary, generally employ interlocking soil-filled reinforced-concrete modules or bins, which resist earth pressures by acting as gravity retaining walls.

Structure Selection

Technical Considerations and Restrictions

MSE Walls MSE walls may be used where conventional gravity, cantilever, or counterforted concrete retaining walls are considered. They are particularly well suited for those locations in which substantial total and differential settlement is anticipated.

Limiting tolerable gradual differential settlement for systems with panels less than 30 ft² in size and a minimum joint width is as follows:

Joint Width (in.)	*Limiting Differential Settlement*
¾	1 in 100 of wall length
½	1 in 200 of wall length
¼	1 in 300 of wall length

When abrupt differential settlement is anticipated (e.g., in the wing walls of culverts and in the culvert itself or in a sudden change of foundation strata), a full-height vertical expansion joint should be incorporated.

The minimum required reinforcing length for both strip and grid reinforcement is 70 percent of the height of the wall. For walls supporting roadways that are deiced with chemicals, an impervious membrane should be placed above the reinforced zone and sloped to a collector drain (Figure 1). For walls constructed in side hill cuts and fill geometries or cuts, a drainage blanket should be constructed to intercept groundwater (Figure 1).

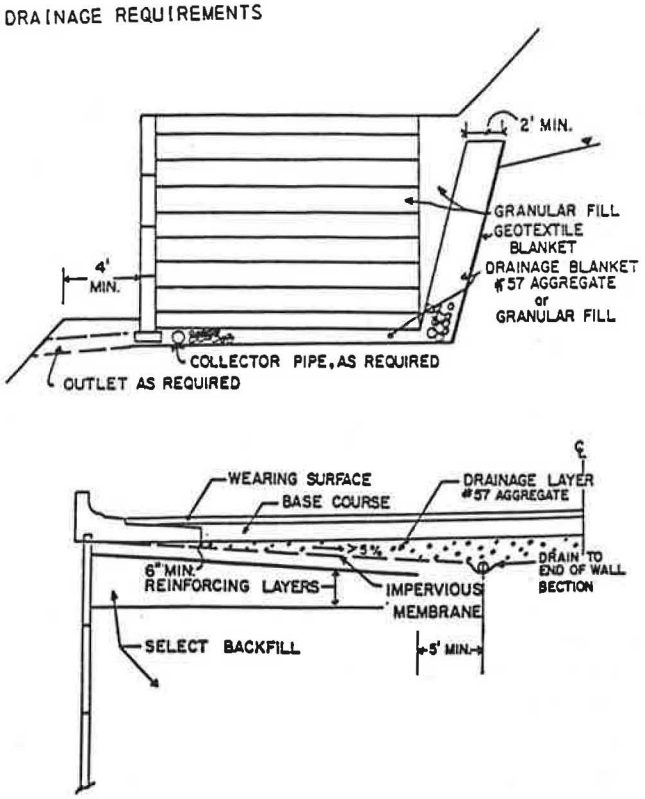

FIGURE 1 Drainage requirements: *top*, drainage blanket detail; *bottom*, impervious barrier detail.

MSE walls should not be used under the following conditions:

- When wall height is greater than 40 ft and mesh reinforcing is used and when wall height is greater than 55 ft and strip reinforcing is used,
- When the groundwater, surface runoff, channel, or stream along the wall is acid contaminated (pH < 6),
- When two intersecting walls form an enclosed angle of 70 degrees or less,
- When utilities other than highway drainage must be constructed within the reinforced zone,
- When differential settlement along the wall is greater than indicated previously in this section,
- When curves have a radius less than 60 ft,
- When floodplain erosion is anticipated to undermine the reinforced fill zone of the wall, or
- When stray ground currents are anticipated within 200 ft of the structure.

Concrete Modular Systems Concrete modular walls are well suited in side-hill cut applications, along stream channels, and where limited space is available to the right-of-way line. When the wall is constructed on fill, the embankment between the original ground and the footing should be composed of granular material or rock.

Concrete Modular Systems should not be used under the following conditions:

- When wall height exceeds 35 ft;
- When the flared wingwalls of abutments are not at 30-degree, 45-degree, or 90-degree angles to the abutment wall or with open-front-face modules;
- When curves have a radius less than 800 ft, unless the curve can be substituted for by a series of chords; or
- When calculated longitudinal differential settlements along the face of the wall are greater than 1 in 200 of the wall length under consideration.

Foundation Submission

The foundation submission report for proprietary walls should include the following:

- Results of all subsurface and laboratory investigations performed to determine allowable bearing pressures;
- Depth of foundations and maximum allowable foundation pressure;
- Necessary foundation improvement techniques, including extent of unsuitable material to be removed;
- Earth pressure coefficients and drainage requirements;
- Systems that will be permitted as alternatives; and
- Maximum estimated settlement during construction and during service life.

The foundation submission is made by the project designer during the design phase of the project.

Design Parameters

Structure Dimensions

All prefabricated walls should be dimensioned to ensure the following factors of safety:

Criterion	*Factor of Safety*
Sliding	>1.5
Overturning on soil	>2.0
Overturning on rock	>1.5
Pullout resistance (MSE walls)	>1.5
wall height ≤ 35 ft	>1.5
wall height > 35 ft	>2.0
Bearing capacity	>3.0
Slope stability	>1.5

Soil reinforcement length should be a minimum of 70 percent of the wall height but not less than 8 ft. For a definition of height for different conditions, see Figures 2 and 3.

Minimum embedment of the wall is as follows:

Slope in Front of Structure	*Minimum Embedment (3-ft min.)*
Horizontal for walls	*H*/20
Horizontal for abutments	*H*/10
3*H*:1*V* for walls	*H*/10
2*H*:1*V* for walls	*H*/7
1.5*H*:1*V* for walls	*H*/5

For walls constructed on slopes, a minimum horizontal bench width of 4 ft width should be provided. For walls constructed along streams, the foundation depth should be established at a minimum of 2 ft below potential scour depth.

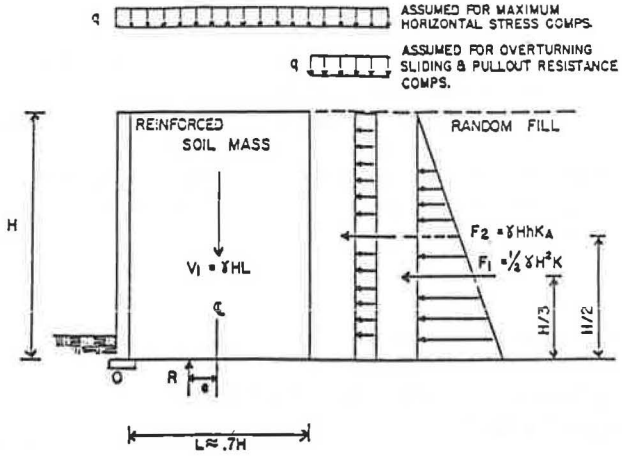

SAFETY FACTOR AGAINST OVERTURNING (MOMENTS ABOUT POINT O):

$$S.F.(O) = \frac{\Sigma \text{ Moments Resisting (Mr)}}{\Sigma \text{ Moments Overturning (Mo)}} = \frac{V_1(L/2)}{F_1(H/3) + F_2(H/2)} \geq 2.0$$

SAFETY FACTOR AGAINST SLIDING:

$$S.F.(S) = \frac{\Sigma \text{ Horizontal Resisting Force(s)}}{\Sigma \text{ Horizontal Driving Force(s)}} = \frac{V_1 \quad \text{Tan}\,\phi}{F_1 + F_2} \geq 1.5$$

ϕ = Friction Angle of Backfill or Foundation, whichever is lowest.

$$e = \frac{L}{2} - \frac{Mr - Mo}{R} \leq \frac{L}{6} \qquad \sigma_v = \frac{R}{L - 2e}$$

where e = eccentricity, q = traffic surcharge, R = resultant of vertical forces V_1, and K_A = see Equation 1

FIGURE 2 Horizontal backslope with traffic surcharge.

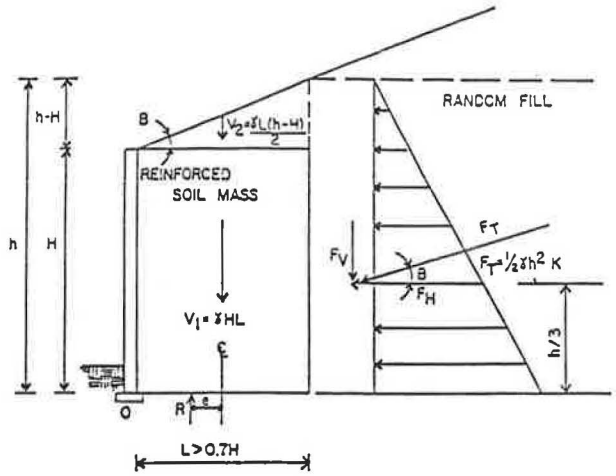

SAFETY FACTOR AGAINST OVERTURNING (MOMENTS ABOUT POINT O):

$$S.F.(O) = \frac{\Sigma \text{ Moments Resisting (Mr)}}{\Sigma \text{ Moments Overturning (Mo)}} = \frac{V_1(L/2) + V_2(2L/3) + F_V(L)}{F_H(h/3)} \geq 2.0$$

SAFETY FACTOR AGAINST SLIDING:

$$S.F.(S) = \frac{\Sigma \text{ Horizontal Resisting Force(s)}}{\Sigma \text{ Horizontal Driving Force(s)}} = \frac{R \text{ Tan}\,\phi}{F_H} \geq 1.5$$

ϕ = Friction Angle of Backfill or Foundation, whichever is lowest.

$$e = \frac{L}{2} - \frac{Mr - Mo}{R} \leq \frac{L}{6} \qquad \sigma_v = \frac{R}{L - 2e}$$

where: e = Eccentricity R = Resultant of vertical forces $V_1 + V_2 + F_V$

FIGURE 3 Sloping backfill case.

External Stability

The external stability of MSE walls should be determined as indicated in Figures 2 and 3. The slope stability should be checked using the Swedish circle or other approved method. See Figure 4 for fill limits.

The coefficient of active earth pressure, K_A, used to compute the horizontal force resulting from random backfill and other factors should be computed on the basis of the friction angle of the random backfill using a Rankine state of stress. Passive pressures should be neglected in stability computations.

$$K_A = \cos B \frac{[\cos B - (\cos^2 B - \cos^2 \phi')^{1/2}]}{[\cos B + (\cos^2 B - \cos^2 \phi')^{1/2}]} \quad (1)$$

where B is the slope angle above the wall, and ϕ' is the internal angle of friction of the random backfill.

The external stability of Concrete Modular Systems should be checked in a manner similar to that for MSE walls. In addition, the Coulomb theory should be used in determining the lateral earth pressure coefficient. The following wall friction angles, δ, should be used unless more exact coefficients are determined:

Case	δ
Significant vibrations of backfill or modules settling more than backfill	0
Continuous pressure surface of precast concrete (uniform-width modules)	$\frac{1}{2}\phi$
Averaged pressure surface (stepped modules)	$\frac{3}{4}\phi$

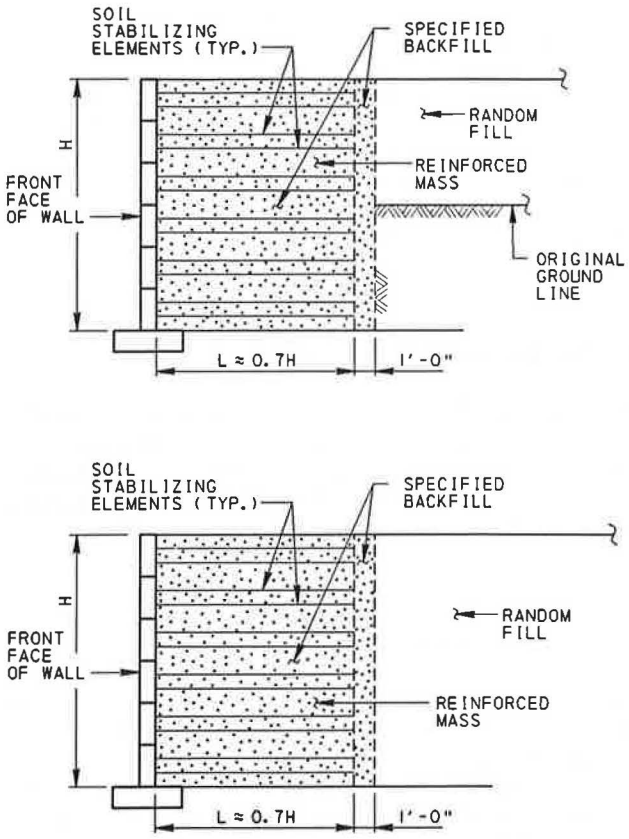

FIGURE 4 Fill limits: *top*, cut-and-fill condition; *bottom*, fill condition.

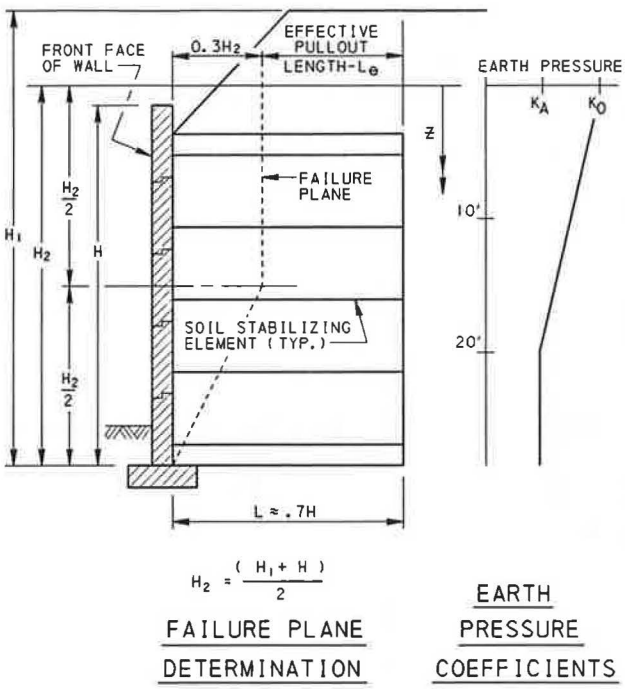

FIGURE 5 Internal stability, MSE walls.

where ϕ is the angle of internal friction of the backfill material behind the wall. Passive pressures should be neglected in stability computations.

Computations for overturning stability should consider that only 80 percent of the soil fill unit weight inside the modules is effective in resisting overturning moments.

Internal Stability

The horizontal stress, σ_H, at each reinforcement level should be computed by multiplying the vertical stress, σ_V, by an earth pressure coefficient, K, shown in Figure 5 where

$$K_A = \tan^2 (45 - \phi/2)$$

$$K_O = 1 - \sin \phi$$

and ϕ is the angle of internal friction of the select backfill.

Pullout Design Parameters

Ultimate pullout capacity of ribbed or smooth steel reinforcing strips is as follows:

$$P_f = f \cdot \gamma \cdot ZA_s \tag{2}$$

where

P_f = pullout capacity per strip,
f = apparent coefficient of friction at each level,
γ = unit weight of soil,
Z = depth to reinforcement, and
A_s = total surface area of reinforcement beyond failure plane.

For ribbed strips, f varies from 1.5 at ground level to the value of tan ϕ at a depth of 20 ft.

For smooth strips, $f = \tan \psi \leq 0.4$, where ψ is the soil reinforcement angle of friction. For fully saturated conditions, site-specific field or laboratory pullout tests should be performed.

For grid reinforcing systems with transverse bar spacing of 6 in. or more,

$$P_p = N_p \cdot Z \cdot \gamma \cdot nA_b \tag{3}$$

where

P_p = ultimate pullout capacity developed by passive resistance per grid,
N_p = passive resistance factor (see Figure 6),
n = number of transverse bearing members behind the failure plane, and
A_b = surface area of transverse reinforcement in bearing (diameter times length).

For grid reinforcements with transverse bar spacing less than 6 in.,

$$P_p = 2 \cdot w \cdot l \cdot \gamma \cdot Z \cdot \tan \phi \cdot f_d \tag{4}$$

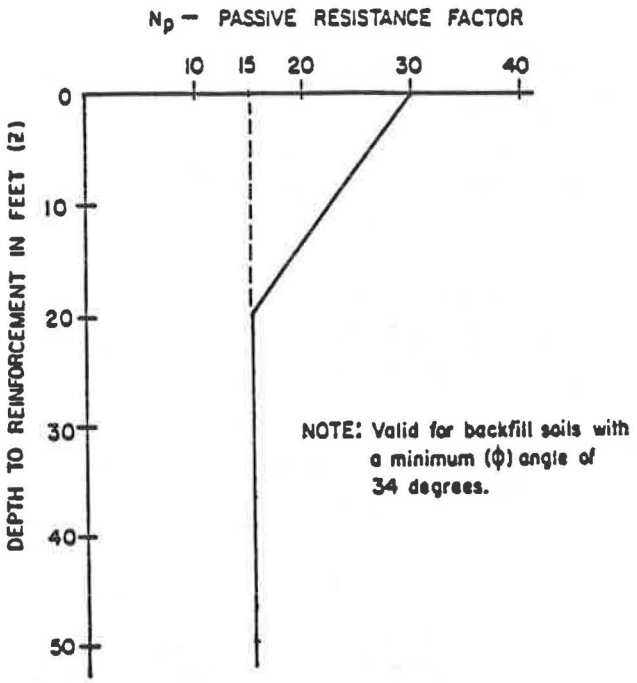

FIGURE 6 Passive resistance factor.

where

w = width of mat,
l = length of mat beyond failure plane,
ϕ = friction angle of soil, and
f_d = coefficient of resistance to direct sliding.

Value varies linearly from 0.45 for continuous sheets to 0.6 for bar mats with transverse spacing of 6 in.

Only the effective pullout length that extends beyond the theoretical failure plane should be used in this computation.

Allowable Stresses and Structural Design

Allowable stresses for MSE walls should be according to AASHTO specifications. For grid reinforcing members, allowable tensile stresses should be reduced to $0.48fy$. Transverse and horizontal grid members should be the same size.

The horizontal force used to design the connections to the panels should not be less than 85 percent of the maximum strip force. However, for structures supporting bridge abutments, full force should be used. The minimum panel thickness should be 5½ in. and the minimum concrete cover should be 1½ in. Epoxy-coated reinforcement bars should be provided where salt spray is anticipated.

Precast Modular Systems should be designed for developed earth pressure behind the wall and for pressure developed inside the modules. The inside pressure (bin) should be the same for each module and less than

$$P_i = \gamma \cdot b \tag{5}$$

where

P_i = inside pressure,
γ = unit weight of soil inside the modules, and
b = width of the module.

Modules should be designed for bending in both vertical and horizontal directions between their supports. Steel reinforcement should be symmetrical on both surfaces unless positive identification of each face can be ensured to preclude reversal of units. Epoxy-coated rebars should be specified when use of deicing chemical sprays is anticipated.

Drainage Requirements

Prefabricated walls in cut areas and side-hill fills with established groundwater levels should be constructed with drainage blankets as shown in Figure 1. For MSE walls supporting roadways that are chemically deiced in the winter, an impervious membrane should be placed as shown in Figure 1.

Design Life Requirements

The soil reinforcement elements in MSE walls should be designed to ensure a minimum design life of 100 years for permanent structures.

The structural design of galvanized soil reinforcements and connections should be made on the basis of a thickness, E_c, defined as follows:

$$E_c = E_n - E_s \tag{6}$$

where E_s is the thickness of metal expected to be lost by uniform corrosion during the service life of the structure, and E_n is the nominal thickness. The sacrificial thickness, E_s, of carbon steel in addition to the galvanization (zinc coating of 2 oz/ft²) for 100 years is 0.05 in.

Special Design Considerations

Special Loading Conditions

Concentrated line loads should be incorporated into the internal design by using a simplified uniform vertical distribution of 2 vertical to 1 horizontal. Traffic loads should be considered in accordance with AASHTO requirements.

In pile-supported abutments constructed on MSE walls, the horizontal forces transmitted to the piles should be resisted by their own lateral capacity or by additional reinforcement in the upper portion of the structure. A minimum clear distance of 1.5 ft should be provided between the facing and the piles. Piles should be driven before wall construction and cased through the fill if necessary. Piles should have corrosion protection in the reinforced zone.

For structures along streams, a differential hydrostatic pressure equal to 3 ft of water should be considered. Buoyant unit weight should be used in the internal and external stability calculations. Seismic design need not be considered unless the acceleration coefficient is greater than 0.1.

Design Details

Parapets should be provided according to PennDOT criteria. When flexible posts and barriers are provided, the upper two rows of reinforcement should be designed for an additional horizontal load of 300 lb/lin ft of wall.

ACKNOWLEDGMENTS

This paper is a condensed version of the Prefabricated Walls portion of the DM-4 (*1*) developed by Victor Elias under the direction of Stephen R. Simco and the authors. The proprietary wall industry's contribution in critiquing the specifications is appreciated. These specifications have been approved by FHWA for use in Pennsylvania. The critique by FHWA is also appreciated.

REFERENCE

1. *Design Manual, Part 4* (DM-4), Volume 1, Parts A and B. Pennsylvania Department of Transportation, Harrisburg, 1988.

Evaluation of Earth Pressures Acting on Slide Suppressor Walls

S. G. WRIGHT, W. M. ISENHOWER, AND M. K. KAYYAL

In Texas, successful repair of shallow slides in earth slopes has been made by embedding retaining walls within the failed slope. Design of these walls requires that the forces exerted on the wall by earth pressures be estimated. Frequently, estimates of the forces must be made with little knowledge of the shear strength properties of the soils involved. This paper presents procedures for calculating forces on the walls using shear strength parameters that are calculated from back-analysis using information pertaining to the original slope when it failed. Simplified procedures are presented that should yield forces nearly as accurate as the forces calculated by much more rigorous procedures.

The Texas State Department of Highways and Public Transportation (SDHPT) has successfully used special retaining "slide suppressor" walls to repair shallow slides in earth slopes. A typical slide suppressor wall is illustrated in Figure 1. The slide suppressor wall consists of a precast panel supported by drilled piers. The wall is placed against the drilled piers, and the piers may contain a semicircular half-section at the point where they support the wall. The slide suppressor wall appears to have been first developed and used by the Texas SDHPT in San Antonio for repair of slides in cut slopes.

The design of the slide suppressor wall requires estimating earth pressure forces that the wall must resist. Conventional earth pressure theories may be used to calculate the earth pressures. Such theories require some knowledge of the shear strength properties of the backfill materials. The backfill material is usually the original slope material, but often there is little information about shear strength properties for design of the wall. In some cases the shear strengths measured in the laboratory may not agree with what is apparently developed in the field. Such inconsistencies between field and laboratory strength values have been found to occur for highly plastic soils used in embankments in Texas [Green and Wright (*1*)].

The long-term shear strength properties, measured using either consolidated-drained or consolidated-undrained test procedures, have been found to be significantly higher than the shear strengths developed in the field. In such cases, use of laboratory shear strength values is unsatisfactory for predicting long-term performance. One way to determine shear strength properties of the slope materials is to calculate the properties from back-analysis using information pertaining to the original slope when it failed.

S. G. Wright and M. K. Kayyal, Department of Civil Engineering, The University of Texas at Austin, Austin, Tex. 78712. W. M. Isenhower, Highway Design Division D-8PD, Texas State Department of Highways and Public Transportation, 11th and Brazos, Austin, Tex. 78701.

Approaches for back-analysis to determine shear strength from slides and to calculate the earth pressure required for design of slide suppressor walls are presented in this paper. Design procedures for the slide suppressor walls themselves are presented by the authors in a companion paper published in this Record.

BACKGROUND

Abrams and Wright (*2*) studied slide suppressor walls and developed a series of charts for computing the forces on walls like the one illustrated in Figure 1. These charts are based on the assumption that a slide has occurred in the slope and this information is used to determine shear strengths by back-analysis. The shear strength parameters determined by back-

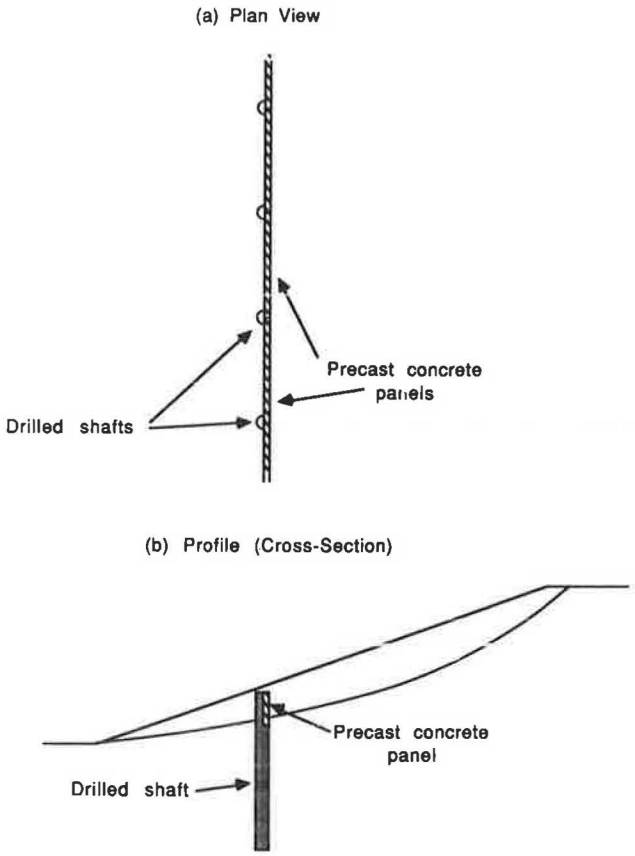

FIGURE 1 Typical slide suppressor wall used for slope repair.

analysis are then used to compute earth pressures for slide suppressor walls.

Shear strengths can be calculated by back-analysis using either a total stress or an effective stress approach. For total stresses the shear strength is expressed as

$$s = c + \sigma \tan\phi \quad (1)$$

where c and ϕ are the cohesion and friction angle, respectively, and σ is the total normal stress on the failure surface.

The shear strength parameters, c and ϕ, can be calculated by back-analysis by knowing (a) the slide geometry and the unit weight of the soil and (b) that the factor of safety is unity (1.0) in a slope that has failed.

Although an infinite number of combinations of c and ϕ theoretically will produce a factor of safety of unity for a slope of a given height and inclination, only one set of values for c and ϕ will also produce a critical shear surface that has the same depth as the observed slide. In general, as the cohesion value increases relative to the friction angle, the depth of slide will increase. Thus, knowing the slope height (H), slope inclination (β), unit weight of soil (γ), and the depth of slide (d), a unique set of values for c and ϕ can be obtained. Any representative definition may be used for the "depth of slide," provided that it is used consistently.

Abrams and Wright (*2*) employed circular shear surfaces, and the depth of slide was defined as the maximum perpendicular distance between the face of the slope and the shear surface, (Figure 2). This measure of the depth of slide is used throughout the following analyses.

When shear strength parameters are calculated by back-analysis using effective stresses, the shear strength is expressed as

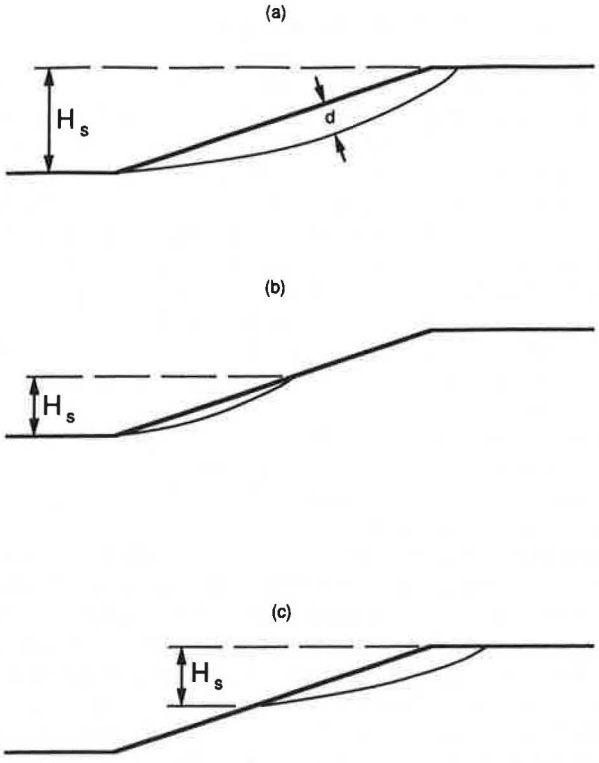

FIGURE 2 Illustration of "depth" and "height" of slide.

$$s = \bar{c} + (\sigma - u) \tan\bar{\phi} \quad (2)$$

where $\bar{c}$ and $\bar{\phi}$ are the cohesion and friction angle, respectively, expressed in terms of effective stresses, and σ and u are the total normal stress and the pore water pressure, respectively, on the failure surface.

To back-calculate effective stress shear strength parameters, the pore water pressure must either be known from measurements or estimated from other information and analyses.

Once shear strength parameters (c and ϕ or $\bar{c}$ and $\bar{\phi}$ are calculated, they can be used to compute the force (P) that would act on a wall extending from the surface of the slope to the shear plane as shown in Figure 3. Different values are calculated for the earth pressures depending on whether the shear strength parameters are expressed using total stresses or effective stresses, and, in the case of effective stresses, on what assumptions are made regarding the pore water pressures.

Abrams and Wright (*2*) studied the differences between earth pressures calculated based on total stresses and effective stresses. For effective stress calculations they assumed several different sets of pore water pressure conditions. In several cases they assumed that the pore water pressures were equal to some constant fraction of the overburden pressure, characterized by values of Bishop and Morgenstern's (*3*) pore pressure coefficient r_u. [The pore pressure coefficient r_u is defined as the ratio of the pore water pressure to the total overburden pressure (i.e., $r_u = u/\gamma z$).] Values for r_u of 0.4 and 0.6 were considered, which represent relatively high values of pore water pressure. Abrams and Wright also considered pore water pressures, which were represented by a relatively high piezometric line in the slope, with at least 80 percent of the soil in the slope located beneath the piezometric line. They found that the differences between the total earth pressures on a wall calculated by effective and total stress procedures were less than 20 percent. The largest differences between earth pressures calculated using total and effective stresses occurred when relatively high values (0.6) were used for r_u. More typical values of pore water pressure produced differences significantly less than 20 percent.

The reason for the relatively small differences in the earth pressures calculated by total and effective stress analyses may be understood by reviewing the effective stress analyses. In the case of effective stress analyses, the highest pore water pressures that are assumed for back-analysis produce the largest values (highest $\bar{c}$ and $\bar{\phi}$) calculated for the shear strength parameters. When these shear strength parameters are used with the corresponding pore water pressures on which they are based, very little difference is found between the total forces on a wall calculated with high pore water pressures and with low pore water pressures. Similarly, little difference is calculated between forces using total stress and any of the effective stress conditions. This observation may only be valid for slopes with a factor of safety of unity, but is applicable to all of those cases of present interest where walls are to be used as remedial measures.

Abrams and Wright (*2*) developed a series of charts for calculating earth pressure forces on slide suppressor walls based on shear strengths calculated by back-analysis of actual slides. They expressed the forces in the form:

$$P = N_P \gamma H_s^2 \quad (3)$$

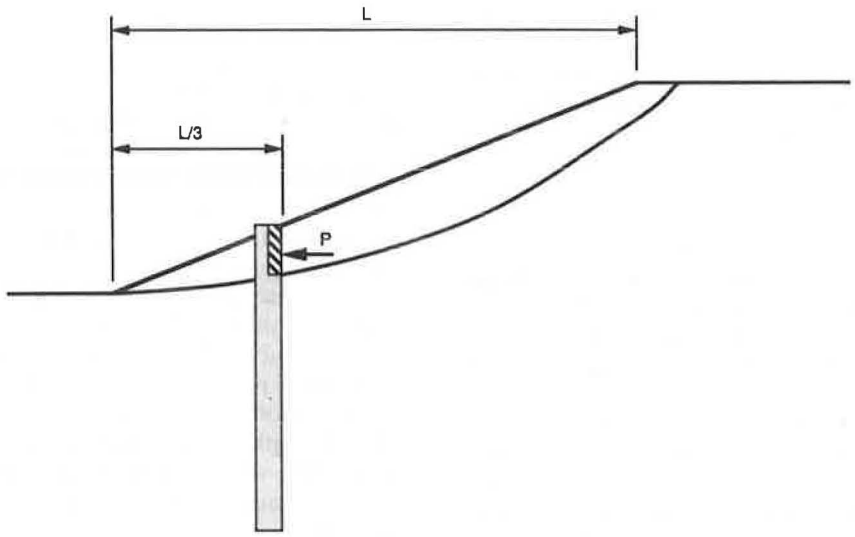

FIGURE 3 Slide suppressor wall and earth pressure force.

where P is the lateral force on the wall, N_P is a dimensionless earth pressure coefficient that depends on the relative depth of the slide (d/H_s), and H_s is the height of the slide. In the case of full-slope failures (Figure 2a) the height of the slide and the height of the slope are the same; however, in the case of partial-slope failures (Figures 2b and 2c), the height of the slide may be less than the slope height. The earth pressure coefficient, N_P, also depends on whether the shear strengths are expressed using effective or total stresses, and in the case of effective stresses, on what assumptions are made concerning the pore water pressures. As discussed earlier, these effects are minor for the present problem. Abrams and Wright plotted charts showing values of N_P versus the relative slide depth (d/H_s) for various slopes, and for both total and effective stresses. A typical chart is shown in Figure 4. This chart was developed using total stresses for a 3:1 slope with the wall located at the lower third point of the slope (Figure 3).

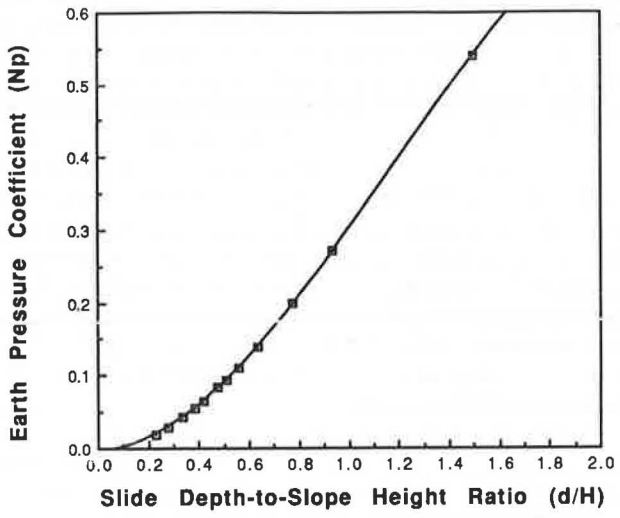

FIGURE 4 Earth pressure coefficients for slide suppressor walls (*2*).

Procedures based on shear strengths determined by back-analysis to calculate earth pressures should provide as good an estimate of the forces on slide suppressor walls as can possibly be made with existing analysis procedures. However, the procedures can be relatively time-consuming to use. The charts developed by Abrams and Wright considerably simplify computations, but the charts encompass only a relatively narrow range of slope, wall, and slide geometries. For most cases the charts cannot be used. In such cases shear strengths must first be calculated by back-analysis and then earth pressures must be calculated.

EFFECT OF SHAPE OF SHEAR SURFACE

Earth pressures are usually calculated using theories based on an assumed shape for the shear surface and satisfying one or more of the equations of static equilibrium. For conventional retaining walls, the shear surface is usually assumed to be planar. However, for slopes that have failed by sliding, the shear surface is seldom planar. Theoretically, the shear surface is more likely to be circular, or, in cases of nonhomogeneous materials, may be some shape other than circular or a simple plane. Abrams and Wright (*2*) employed circular shear surfaces to calculate the earth pressures on slide suppressor walls using a procedure based on an extension of Spencer's procedure of slices (*4*). The procedure satisfies all requirements of static equilibrium. The procedure should be more correct than the classical earth pressure theories (which are restricted to a planar shear surface and do not explicitly satisfy moment equilibrium).

Approaches based on Spencer's procedure of slices are fundamentally more correct than simpler procedures to calculate earth pressures on walls embedded in slopes. However, the procedures are relatively cumbersome to use and require a computer program to implement. A computer program was developed and used by Abrams and Wright to perform the earth pressure calculations; however, this program has not been maintained. To the author's knowledge, no computer program is currently generally available for computing earth

pressures employing Spencer's procedure of slices. For most practical cases it is desirable to use simpler procedures to calculate the earth pressures, especially when conditions are outside the range of the charts developed by Abrams and Wright.

To examine the feasibility of using simpler approaches to calculate earth pressures on slide suppressor walls, forces were calculated using two procedures: (a) Spencer's procedure with circular shear surfaces, and (b) the classical "trial wedge" earth pressure theory employing planar shear surfaces. Calculations were performed for seven slides for which data are summarized in Table 1. Five of the seven slides (1, 2, 3, 4, and 7) selected for study occurred in cut slopes; the remaining two slides (5 and 6) occurred in fill slopes. Measured and/or estimated dimensions of the slides are shown in Table 1. In all cases the total unit weight of soil was assumed to be 125 pcf.

In Texas, experience with shallow slides in embankments, as well as with many cut slopes, suggests that the pore water pressures in the slopes are negligible (Stauffer and Wright (*5*)). Many of the soils involved are highly desiccated and failures have occurred during wet periods due to surface water infiltration and soil expansion. However, there appears to be little evidence of significant positive pore water pressures. Accordingly, calculations were performed for the seven slides summarized in Table 1, assuming that the pore water pressures were zero. In this case, there was no difference between effective stresses and total stresses.

Calculations were performed for the forces on slide suppressor walls located at a point one-third of the distance from the toe of the slope to the crest, as shown in Figure 3. The walls were assumed to extend vertically from the surface of the slope to the slide surface. Earth pressures based on Spencer's procedure were calculated using the charts developed by Abrams and Wright. For the trial wedge procedure the shear strength parameters were calculated using the known slide geometry and Spencer's procedure of slope stability analysis. This is the same procedure used by Abrams and Wright to calculate shear strengths and, accordingly, the shear strength parameters are identical. The calculated shear strength parameters (c and ϕ) are included in Table 1.

The earth pressure forces calculated using Spencer's procedure and the trial wedge procedure are summarized in Table 2. In all but one case, the earth pressures based on Spencer's procedure were slightly larger, probably due to the fact that the forces are based on a more critical shear surface (circular versus planar). In the one case where Spencer's procedure yielded a lower force, the difference is believed to be due to the difficulty in reading values precisely from Abrams and Wright's charts. In all cases, the differences between the two sets of earth pressures shown in Table 2 are considered insignificant. Accordingly, it appears that planar shear surfaces can be used for computations of earth pressures on slide suppressor walls.

INFLUENCE OF COHESION VALUE

The cohesion values, which were calculated and summarized in Table 1 for the seven slides, are all relatively small. This is typical of shallow slides like those shown in Table 1 where the slide depth-to-height ratio (d/H_s) is approximately one-third or smaller. This suggests that shear strengths could be calculated by assuming zero cohesion and by calculating the friction angle corresponding to a factor of safety of unity. In such cases, the friction angle is simply equal to the slope angle (i.e., $\phi = \beta$).

Although not shown directly in Table 2, the previous calculations also revealed that the assumed distance that the backfill extended behind the wall had a relatively minor effect on the earth pressure force and, thus, the distance may be unimportant. To illustrate the effect of the extent of the backfill, calculations were performed using the two sets of slope and soil properties shown in Table 3. The distance between the wall and the horizontal ground surface (w) was varied from a value equal to the height of the wall to values much

TABLE 1 INFORMATION FOR SLIDES USED IN STUDIES

Slide No.	Location	Slope Ratio	Height of Slide (ft)	Depth of Slide (ft)	Cohesion (psf)	Friction Angle (degs)
1	US 75 at Lamberth Road Northeast Quadrant	2:1	22	4.5	17	19
2	US 82 and FM 131 Southeast Quadrant	3:1	14	5	18	51
3	US 82 and FM 131 Southwest Quadrant	3:1	13	3	5	17
4	US 75 North and FM 691 West Side	3:1	6	2	6	15
5	South US 82 @ M & P Railroad	3:1	24	4.8	6	17
6	US 271 @ Stillhouse Road	2.5:1	13	2	2.3	21
7	US 271 @ B & N Railroad	3:1	14	2.5	2.5	17

TABLE 2 COMPARISON OF EARTH PRESSURE FORCES CALCULATED USING TRIAL WEDGE AND SPENCER'S PROCEDURES

Slide No.	Force - Trial Wedge (lbs)	Forces - Spencer's Procedure (lbs)	Difference[1] (percent)
1 (r_u = -0.2)	785	941	- 17
1 (r_u = 0)	824	941	- 12
2	1074	1159	- 7
3	409	456	- 10
4	155	184	- 16
5	1023	1123	- 9
6	197	211	- 7
7	295	254	16

$$^{1}\text{Percent Difference} = \frac{P_{\text{Trial Wedge}} - P_{\text{Spencer's}}}{P_{\text{Spencer's}}} \times 100\%$$

TABLE 3 PARAMETERS USED IN STUDIES TO ILLUSTRATE EFFECT OF THE EXTENT OF THE BACKFILL SLOPE

Parameter	Case I	Case II
Wall height, h	10 ft.	5 ft.
Slope angle, β	20°	18.4° (cot β = 3.0)
Unit weight of soil, γ	125 pcf	125 pcf
Cohesion, c	0	10 psf
Friction angle, f	20°	15°

greater than the height of the wall (Figure 5). The earth pressure forces for the two sets of parameters are plotted versus the extent of the backfill in Figure 6. For illustrative purposes the distance, w, has been normalized by dividing it by the height of the wall, h. For both cases the extent of the backfill slope has only a moderate influence on the forces and is insignificant when the backfill extends behind the wall a distance equal to more than five times the wall height.

The above observations indicate that the earth pressure forces could be calculated based on the assumption of a just-stable, cohesionless backfill, extending an infinite distance behind the wall, and using a planar shear surface. Earth pressure forces calculated by this simplified procedure are compared in Table 4 with those calculated employing Spencer's procedure and the shear strength parameters (c and ϕ) summarized in Table 1. Earth pressures by the simplified procedure were calculated for a planar shear surface using both Coulomb and Rankine classical earth pressure theories. For the Coulomb theory the earth pressure force is assumed to act horizontally on the wall; for the Rankine theory the earth pressure force is assumed to act parallel to the slope. (Assumption of an earth pressure force acting parallel to the ground surface in the Coulomb theory will produce results identical to those by the Rankine theory). These two assumptions for the inclination of the resultant earth pressure force should bracket the probable inclinations of the earth pressure force. The backfill slope was assumed to be infinite (i.e., the backfill extended an infinite distance behind the wall with no horizontal ground surface). The results of the calculations summarized in Table 4 show that the differences between the earth pressures computed by the rigorous and simplified approaches are usually no larger than 12 percent and could be considered negligible for practical purposes. Abrams and Wright's charts were used to perform the calculations by the rigorous procedure. For the one case where larger differences are shown

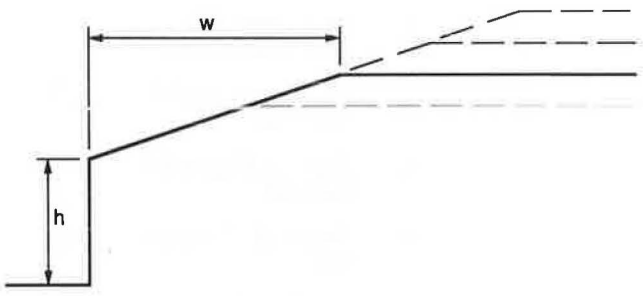

FIGURE 5 Illustration of extent of backfill varied for parametric study.

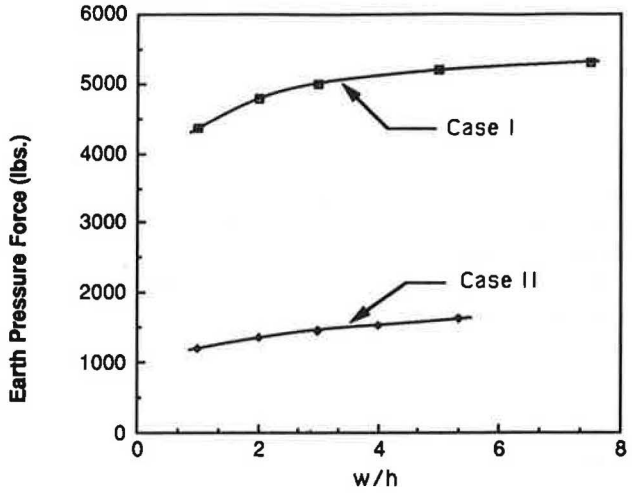

FIGURE 6 Variation in earth pressure force with extent of backfill.

(Slide 7), the differences are believed to be due to difficulties encountered with accurately picking values of the coefficient N_P from Abrams and Wright's charts. Selection of precise values from the charts was difficult for very small slide depth-to-height ratios.

FURTHER SIMPLIFICATION OF PROCEDURES

Examination of the earth pressures shown in Table 4 suggested that even further simplification of the procedures is possible. Active earth pressure coefficients, K_A, were calculated for a cohesionless material with a backfill sloping at the same angle as the angle of internal friction for the soil. The earth pressure coefficients calculated in this manner correspond to earth pressures calculated using the simplified procedures described in the previous section. The coefficients were calculated using the expression

$$P = \frac{1}{2}K_A\gamma h^2 \tag{4}$$

where P is the earth pressure force calculated by the simplified procedures. The earth pressure coefficients were calculated for both Rankine and Coulomb earth pressure theories. In the case of the Coulomb theory, the earth pressures were assumed to act in the horizontal direction. The earth pressure coefficients are plotted in Figure 7.

The earth pressure coefficients in Figure 7 show that for slopes 2:1 or flatter (slope angle less than 26.5 degrees) the earth pressure coefficient is at least 0.8 and in many cases 0.9 or larger. Thus, the earth pressures are within 20 percent of what they would be if the wall were assumed to be backfilled with a fluid having the same unit weight as the soil. The differences between the pressures calculated by earth pressure theories and those for an equivalent fluid would be expected to be even smaller if curved, rather than planar, shear surfaces had been assumed. Consequently the differences are minor and for design of slide suppressor walls in slopes which have failed or are barely stable, the backfill can be assumed to act as a fluid.

TABLE 4 COMPARISON OF EARTH PRESSURE FORCES CALCULATED USING RIGOROUS PROCEDURE AND TRIAL WEDGE PROCEDURE ASSUMING JUST-STABLE COHESIONLESS BACKFILL SLOPE

	Rigorous	Coulomb Theory		Rankine Theory	
Slide No.	Procedure	Force	Difference[1]	Force	Difference[2]
	(lbs)	(lbs)	(%)	(lbs)	(%)
1	941	841	-11	940	≈ 0
2	1159	1089	- 6	1148	- 1
3	456	410	-10	432	- 5
4	184	163	-12	171	- 7
5	1123	1040	- 7	1096	- 2
6	211	195	- 8	209	- 1
7	254	298	17	314	23

$$^1\text{Percent Difference} = \frac{P_{Coulomb} - P_{Rigorous}}{P_{Rigorous}} \times 100\%$$

$$^2\text{Percent Difference} = \frac{P_{Rankine} - P_{Rigorous}}{P_{Rigorous}} \times 100\%$$

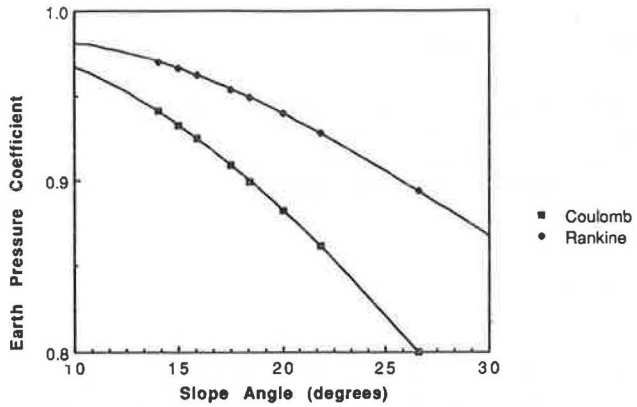

FIGURE 7 Earth pressure coefficients for just-stable cohesionless backfill.

SUMMARY AND RECOMMENDATIONS

Design of slide suppressor walls to be installed in slopes that have experienced shallow slides can be based on shear strength parameters calculated by back-analysis of the slide. Results of this study show that for slide depth-to-height ratios (d/H_s) of one-third or less the shear strengths can be calculated assuming that the backfill is cohesionless. In the case of a just-stable slope and cohesionless backfill the angle of internal friction, ϕ, is equal to the slope angle, β.

The studies also show that for just-stable backfills in cohesionless materials, the earth pressure coefficient for most of the slopes of interest (2:1 or flatter) will be within 20 percent, and often 10 percent, of unity, indicating nearly hydrostatic stresses. Accordingly, for design of walls in marginally stable slopes, where the slide depth and wall height do not exceed one-third of the height of the slide, an earth pressure coefficient of unity can be assumed. Thus, the earth pressures for walls embedded in the slope can be computed from

$$P = \frac{1}{2}\gamma h^2 \tag{5}$$

where h represents the wall height, assuming that the wall extends from the ground surface downward. If the top of the wall is below the ground surface, h should represent the depth from the ground surface to the bottom of the wall. The expression given by Equation 5 should be valid for walls embedded up to one-third the height of the slide ($h \leq H/_s^3$). This range in depths (0 to $H/_s^3$) covers a large number of the slides in highway cuts and embankments in Texas.

ACKNOWLEDGMENT

The authors wish to express their thanks to Bobby L. Myers, District Engineer of the Texas SDHPT District 1, Paris, Texas, for his support and encouragement of the work presented in this paper.

REFERENCES

1. R. Green and S. G. Wright. Factors Affecting the Long Term Strength of Compacted Beaumont Clay. *Research Report 436–1*. Center for Transportation Research, The University of Texas at Austin, Oct. 1986.
2. T. G. Abrams and S. G. Wright. A Survey of Earth Slope Failures and Remedial Measures in Texas. *Research Report 161–1*. Center for Highway Research, The University of Texas at Austin.
3. A. W. Bishop and N. Morgenstern. Stability Coefficients for Earth Slopes. *Geotechnique*, Vol. 10, No. 4, Dec. 1960, pp 129–150.
4. E. Spencer. A Method of Analysis of the Stability of Embankments Assuming Parallel Inter-Slice Forces. *Geotechnique*, Vol. 17, No. 1, Mar. 1967, pp 11–26.
5. P. A. Stauffer and S. G. Wright. An Examination of Earth Slope Failures in Texas. *Research Report 353–3F*. Center for Transportation Research, The University of Texas at Austin, Nov. 1984.

Design Procedures for Slide Suppressor Walls

W. M. ISENHOWER, S. G. WRIGHT, AND M. K. KAYYAL

A slide suppressor wall is a retaining wall that is embedded in a slope that has failed. Slide suppressor walls are used to repair shallow slope failures in areas where right-of-way is restricted and the slope cannot be flattened. The design procedure for slide suppressor walls assumes that earth pressure acting on the wall is equal to a hydrostatic pressure of a fluid with a density equal to the total unit weight of soil. The performance of the supporting drilled shafts and load-carrying capacity of the wall panels were evaluated for a range of wall geometries. Design charts for walls supported by 18-in. and 24-in. shafts are presented. A cost study found that slide suppressor walls cost about $10 to $18/ft² and are more economical than conventional earth-retaining structures.

This paper presents a procedure developed by the Texas State Department of Highways and Public Transportation (SDHPT) for the design of "slide suppressor" walls. This design procedure is based on a simplified method for estimating the magnitude of earth pressures acting on a wall. The method used to estimate the earth pressures acting on a slide suppressor wall is reviewed. This is followed by a discussion of (a) the analysis of the wall slabs and supporting drilled shafts, (b) the selection of the size of wall slabs, and (c) spacing between the drilled shafts. Finally, a comparison is made between the costs of slide suppressor walls and conventional retaining walls.

BACKGROUND

The stability of embankments and cut slopes in highly plastic clays has been a continuing maintenance problem in Texas. Many reasons for the problem exist; however, only a few can be effectively addressed by state officials. In areas where slope maintenance costs are high, two causes of the problem stand out. One is the poor quality of soil encountered. Texas has large expanses of highly plastic, expansive clays that have low drained friction angles (commonly between 12 degrees and 20 degrees) and negligible effective cohesion. A second cause is the influence of the weather on the poor-quality soils across the state. A soil deposit might cause significant problems in areas where the winter season brings high rainfall and many freeze-thaw cycles, and cause fewer problems in areas with a more moderate climate.

The areas with the greatest problems have the following features in common:

- Expansive clays,
- Wet winters with many freeze-thaw cycles,
- Dry summers with little rain, and
- Moderate (3 horizontal to 1 vertical) to steep slopes.

The variation in weather over a year causes the clays to expand when wet and to crack when dry. With later cycles of wetting and drying, the zone of cracking and weathering extends deeper into the fill or cut. About 10 to 30 years after construction, the clay has "decompacted," becoming loose and having a low shear strength. Later, usually during a period of continual rainfall in early winter, the clay becomes saturated and a shallow mud-flow, face-failure occurs on the slope.

While many slides have occurred in slopes steeper than 3 horizontal to 1 vertical, many slides have also occurred in slopes that are close to this steepness. This is surprising since a slope stability analysis can show that a slope in "normal soil," with the expected range in shearing properties, should have an adequate factor of safety against failure. Studies of slope failures have found that the shear strength values back-calculated from slope failures are lower than those measured on laboratory-prepared samples of the same soils (*1,2*). In addition, many failures do not extend beyond the toe and crest of the slope. This type of failure geometry is characteristic of soils with low cohesion values. The occurrence of the failures is direct proof that the shearing properties of the soils have altered, with effective cohesion approaching zero and effective friction angles increasing somewhat, and that weathering has an effect that is dependent on the prevailing climatic conditions.

If an adequate amount of right-of-way is available, the most economical way to stabilize slope failures is to flatten the slope. In areas where restricted right-of-way prevents flattening of the slope, Texas SDHPT has used slide suppressor walls to remedy slope failures. A slide suppressor wall is a retaining wall buried in the slope. Typically, the slide suppressor wall is located at one-third of the slope height as illustrated in Figure 1. Because it is embedded, the wall can mobilize the sliding resistance of the downslope soils and needs only to add enough additional resistance against sliding to provide stability. The embedment of the wall allows the wall to be lighter in section than a conventional retaining wall and thereby less expensive to construct.

Slide suppressor walls have several advantages over conventional retaining structures. The most important advantage is cost. Slide suppressor walls can be built for about 50 to 60 percent of the cost of a conventional retaining structure. A second advantage is that it is possible to construct the walls quickly by using prefabricated wall sections. A third advan-

W. M. Isenhower, Highway Design Division D-8PD, Texas State Department of Highways and Public Transportation, 11th and Brazos, Austin, Tex. 78701. S. G. Wright and M. K. Kayyal, The University of Texas at Austin, Austin, Tex. 78712.

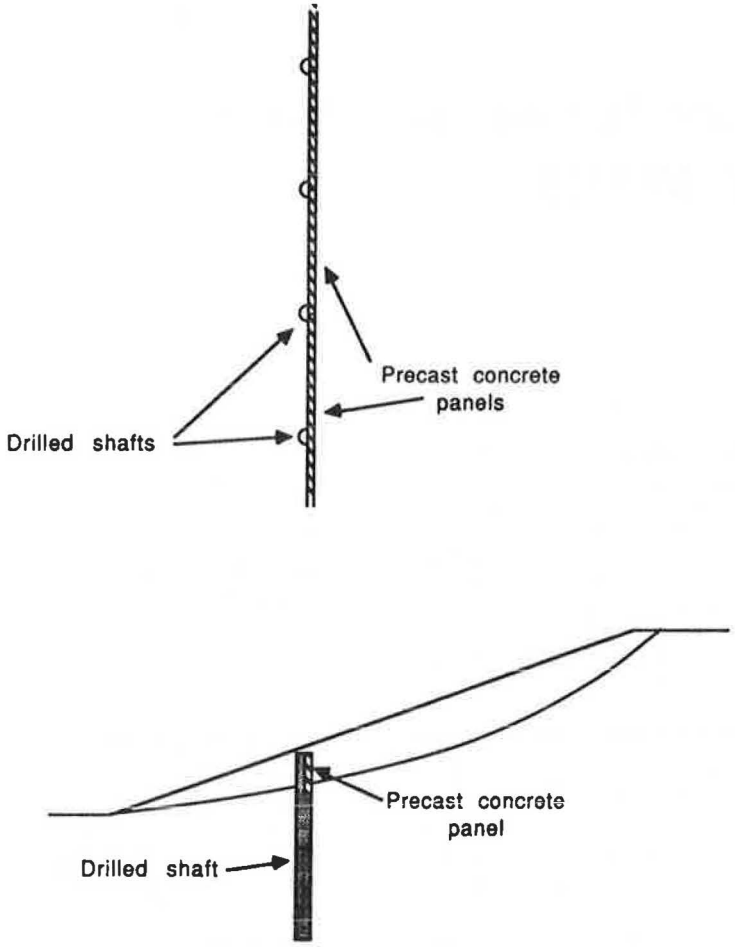

FIGURE 1 Typical slide suppressor wall used for slope repair: *top*, plan view; *bottom*, profile (cross section).

tage is that after wall construction, the slope geometry closely resembles that of the original slope and access is unrestricted for mowing and other maintenance.

The design procedure presented in this paper is intended for use by personnel who are not geotechnical specialists. These personnel will not have conducted a geotechnical investigation beyond determining the depth of slide and determining the Atterberg limits of the soils in the slope. As a result, several conservative assumptions related to the earth pressure calculations and soil properties have been made. The purpose for the discussion of the methods used to develop the design procedure is to guide the reader in designing slide suppressor walls whenever more detailed information is available.

CALCULATION OF EARTH PRESSURES

The development of the method used to calculate the earth pressures acting on a slide suppressor wall is discussed by the authors in a companion paper in this Record. The earth pressures acting on walls installed in slopes that have failed can be calculated, for all practical purposes, assuming that the soil is cohesionless. For a just-stable (i.e., factor of safety = 1), cohesionless soil, the angle of internal friction is equal to the slope angle. The companion paper found that the earth pressure coefficient will be within 20 percent of unity, and will be within 10 percent of unity for slope angles of less than 20 degrees. These values suggest that the earth pressures acting on a slide suppressor wall are nearly hydrostatic. For purposes of wall design in marginally stable slopes, the earth pressure coefficient of unity was assumed. Thus, the earth pressure per unit width (P) acting on a slide suppressor wall built at one-third of the slope height is computed from

$$P = \frac{1}{2}\gamma h^2 \tag{1}$$

where γ is the total unit weight of the soil and h is the depth of embedment.

The depth of embedment is selected on consideration of the depth of the slide observed in the field. Typically, a wall height is set equal to the depth of slide plus about 1 ft. If the depth of slide is deep and not a shallow failure, a general slope failure is likely, and a slide suppressor wall may be inadequate for repair.

WALL PANELS

The wall panels of the slide suppressor walls are constructed using prestressed concrete slabs. The details for these slabs

were selected from the solid flat slabs presented in the *PCI Design Handbook* (*3*). Solid flat slabs with thicknesses of 4 in., 6 in., and 8 in. were considered. In determining the load-carry capacity of a slab, the safe superimposed service loading on a slab was increased over the value shown in the handbook by the amount of the dead load for each slab. The reason for this increase is that the wall slabs will be buried and will not have to support the dead loads of 50 psf for a 4-in. slab, 75 psf for a 6-in. slab, and 100 psf for an 8-in. slab.

The allowable bending moments in the slabs were calculated from the safe superimposed service load plus dead load values for each combination of slab length and slab height. The maximum bending moment was calculated using

$$M_{max} = \frac{w\,l^2}{8} \tag{2}$$

where w is the average load per unit area and l is the length between supporting drilled shafts. A summary of the allowable bending moments calculated for 4-, 6-, and 8-in.-thick slabs is shown in Table 1.

The maximum bending moments in the wall slabs are dependent on the magnitude of the average earth pressure acting on the wall and the span between the supporting drilled shafts. The maximum bending moments in the wall were calculated using the assumption that the soil acts as a fluid with a density equal to the total unit weight of 125 pcf. The maximum bending moments for different size wall panels are shown in Table 2. No moments are shown in Table 2 for the cases where the maximum bending moment will exceed the capacity of the strongest 8-in. slab. The information in Tables 1 and 2 was combined to determine the slab thickness and reinforcement strand pattern designation for several combinations of panel length and height. Tables 3 through 5 show the reinforcement strand pattern designations for the various combinations of panel length and panel height for each wall thickness.

The reinforcement strand pattern designation is a description of the amount and size of reinforcement in the slab. The tens digit designates the number of strands per foot width of slab. The ones digit designates the diameter of the strand in 16ths of an inch. The suffix S designates that the strands are

TABLE 1 ALLOWABLE BENDING MOMENTS IN WALL PANELS

Strand Pattern Designation	Allowable Bending Moment[a] ft-lb		
	Wall Thickness in Inches		
	4	6	8
66-S	2713	5309	8967
76-S	3088	5702	9947
58-S	3788	5793	10094
68-S	4263	5884	10241
78-S		5974	11166

[a]from safe superimposed service load plus dead load, $f'_c = 5000$ psi, low-relaxation strand

TABLE 2 MAXIMUM BENDING MOMENTS IN WALL PANELS PER WALL HEIGHT

Panel Length ft	Maximum Bending Moments ft-lb							
	Wall Height in Feet							
	3	4	5	6	7	8	9	10
9	1898	2531	3164	3797	4430	5063	5695	6328
10	2344	3125	3906	4688	5469	6250	7031	7813
11	2836	3781	4727	5672	6617	7563	8508	9453
12	3375	4500	5625	6750	7875	9000	10125	
13	3961	5281	6602	7922	9242	10563		
14	4594	6125	7656	9188	10719			
15	5273	7031	8789	10547				
16	6000	8000	10000					
17	6773	9031						
18	7594	10125						
19	8461							
20	9375							

TABLE 3 SOLID FLAT SLAB STRAND PATTERN DESIGNATION FOR 4-IN. WALL PANELS (TYPE FS4)

Panel Length ft	Strand Pattern Designation							
	Wall Height in Feet							
	3	4	5	6	7	8	9	10
9	66-S	66-S	58-S	68-S				
10	66-S	58-S	68-S					
11	76-S	58-S						
12	58-S							
13	68-S							

TABLE 4 SOLID FLAT SLAB STRAND PATTERN DESIGNATION FOR 6-IN. WALL PANELS (TYPE FS6)

Panel Length ft	Strand Pattern Designation							
	Wall Height in Feet							
	3	4	5	6	7	8	9	10
9					66-S	76-S	76-S	
10				66-S	76-S			
11			66-S	76-S				
12		66-S	76-S					
13		66-S						
14	66-S							
15	66-S							

TABLE 5 SOLID FLAT SLAB STRAND PATTERN DESIGNATION FOR 8-IN. WALL PANELS (TYPE FS8)

Panel Length ft	Strand Pattern Designation							
	Wall Height in Feet							
	3	4	5	6	7	8	9	10
9								66-S
10						66-S	66-S	66-S
11					66-S	66-S	66-S	76-S
12				66-S	66-S	76-S	68-S	
13			66-S	66-S	76-S	78-S		
14		66-S	66-S	76-S	78-S			
15		66-S	66-S	78-S				
16	66-S	66-S	58-S					
17	66-S	76-S						
18	66-S	68-S						
19	66-S							
20	76-S							

straight in the slab. The strands have a 1.5-in. of cover on the tension side of the slab and are made of low-relaxation steel. The compressive strength of the concrete is 5,000 psi.

ANALYSIS OF DRILLED SHAFT BEHAVIOR

The objective of the analysis of drilled shaft behavior was to establish a relationship between the depth of shaft required to support the wall adequately given the height of wall and pressure acting on the wall. This relationship is used in the cost analysis to select the depths of shafts required to support wall panels of various lengths.

The analysis of the supporting drilled shafts took two steps. The first step was to evaluate the nonlinear bending stiffness and maximum allowable bending moment for the drilled shafts being considered. The second step was to analyze the performance of drilled shafts subjected to a distributed lateral load that modeled the loading on a slide suppressor wall. Calculation of the nonlinear bending stiffnesses of the various size of shafts used in the study were made using STIFF1 (*4*). Analyses of the laterally loaded drilled shafts were made using LPILE1 (*5*).

Bending Stiffness of Shafts

The analysis of laterally loaded drilled shafts requires values for moment of inertia and modulus of elasticity to calculate the bending stiffness of the shafts. For steel piles, the modulus of elasticity is well known and the moments of inertia for standard shapes can be found in steel design handbooks. In contrast, no comparable reference is available for concrete shafts because of the wide variation in material properties and structural details.

The bending stiffness of a drilled shaft depends on the compressive strength of the concrete, yield strength of the reinforcing steel, the arrangement of reinforcement, the combination of axial load and bending moment, and whether the section is cracked in the zone of tension. STIFF1 calculates the bending stiffness taking the above features into account.

The nonlinear bending stiffnesses for 18-in. and 24-in. drilled shafts are shown as a function of maximum concrete strain in Figures 2 and 3. These shafts have a compressive strength of

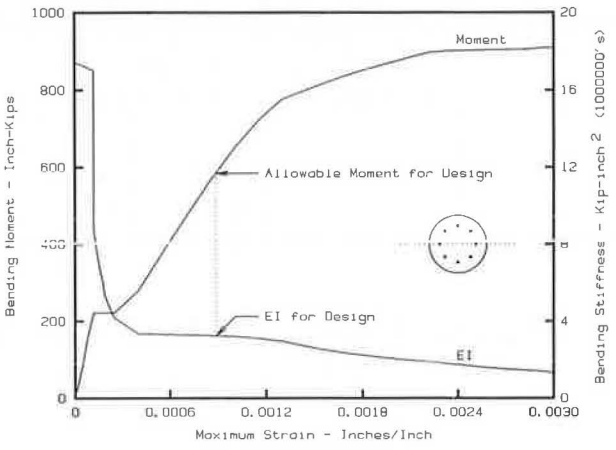

FIGURE 2 Eighteen-in. drilled shafts with 1 percent 60-ksi reinforced steel.

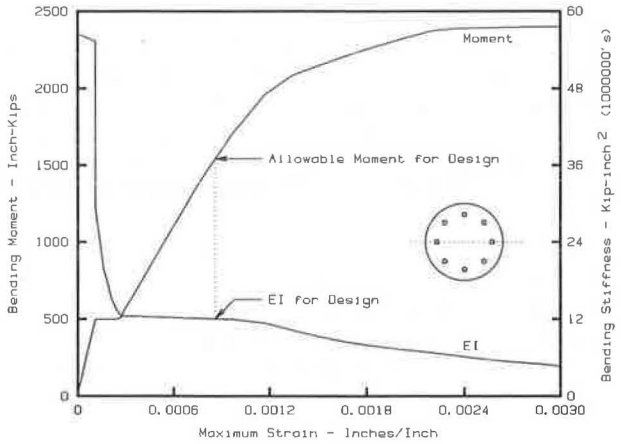

FIGURE 3 Twenty-four-in. drilled shafts with 1 percent 60-ksi reinforced steel.

concrete equal to 3,000 psi and have steel reinforcement equal to 1.0 percent of the gross area. The yield strength of the reinforcing steel is 60 ksi. The clear cover over the reinforcing steel is 3 in. The arrangement of the reinforcement is shown in Figures 2 and 3.

The value of bending stiffness used in the lateral loading analyses was the value corresponding to the maximum allowable bending moment. The maximum allowable bending moment was at a maximum strain of 0.003 in./in., reduced by a strength reduction factor of 0.9, divided by a load factor of 1.4 for dead load, and with the live loading component considered to be zero. The maximum allowable bending moment, bending stiffness, moment of inertia, and equivalent modulus of elasticity for the shafts considered are shown in Table 6.

Lateral Loading Analyses

The analysis of the performance of drilled shafts subjected to lateral loading was made using LPILE1. This program can analyze a shaft subjected to general pile-head loading (shear force, axial loading, and bending moment) and distributed lateral loading over a selected section of the shaft. This program is also capable of using soils data to generate the lateral load-transfer curves (p-y curves) used in the analysis.

The objective for the analysis of drilled shaft behavior was to establish the general relationship between the depth of shaft required to support a wall of a given height and the level of lateral loading acting on the drilled shaft. The purpose was to determine if it is possible to overload the drilled shafts by using wall panels that are too long, thereby exerting high levels of lateral loading on the drilled shafts. The procedure

TABLE 6 STRUCTURAL PROPERTIES OF DRILLED SHAFTS

Shaft Diameter inches	Allowable Moment in-lb	Bending Stiffness $lb\text{-}in^2$	Moment of Inertia in^{4*}	Modulus of Elasticity psi**
18	546000	3220000000	5153	625000
24	1389000	12110000000	16286	744000

* Calculated from gross area of shaft
** E = EI/I

was to analyze a drilled shaft subjected to four or five levels of lateral loading distributed over the upper section of the shaft where the wall is supported. In these analyses, the depth of slide and the wall height were assumed to be equal. For each level of loading that did not overstress the shaft, the depth of shaft required to carry that level of loading was equal to the depth of the second inflection point of deflection. Figure 4 shows the results of one such analysis on a drilled shaft supporting a 5-ft-high wall. Figure 4 demonstrates that both bending moment and lateral deflection become negligible below the depth of the second inflection point of deflection.

After the required shaft depths were obtained for several loadings on wall heights varying from 3 to 10 ft, a least-squares curve was fit through the data. This related shaft depth to wall height and level of distributed lateral load for all analyses in which the shafts were not overstressed. This relation was developed to allow the user to estimate the shaft depths required to support walls subjected to loads smaller than the maximum shaft capacity.

The procedure presented above was made for 18-in. and 24-in. diameter drilled shafts constructed with concrete with 3,000 psi compressive strength and a 3-in. cover over 1.0 percent 60-ksi steel. Larger amounts of reinforcement were examined initially but were found to have negligible influence based on the criteria of a shaft depth with two inflection points of deflection.

In all analyses the Matlock criteria (*6*) for p-y curves for pile in soft clay was used with an undrained shear strength value of 1,000 psf. The soft clay p-y criteria was selected instead of criteria for stiff clay so that the initial slope of the p-y curve could model long-term loading conditions. Broms (*7*) has suggested that the long-term increase in shaft deflections due to consolidation and creep of soil may be calculated by assuming subgrade reactions that are one-half to one-quarter of the initial values for static loading. Undrained shearing strength of highly plastic clay fills typically range from about 2,000 to 2,200 psf. By using the soft clay p-y criteria and an undrained shearing strength of 1,000 psf one may obtain a p-y curve with an initial slope that is about 43 percent (1/2.34) of the initial slope of a p-y curve calculated using the stiff clay above the water table criteria.

The analysis of the drilled shafts produced two results. The first result is the limiting level of distributed load for each wall height (assumed to be equal to the depth of slide) below which loading must be kept to avoid overstressing the drilled shafts. The second result is a relationship for the shaft depth required for two inflection points of deflection as a function of slide depth and distributed load for distributed loads below the maximum allowable load on a shaft. The maximum allowable distributed loads as a function of depth of slide for 18- and 24-in. shafts are shown in Figure 5.

None of the wall panels shown in Tables 3 through 5 is strong enough to carry a load equal to the load of the limiting soil pressures shown in Figure 5. The loading on the shafts, therefore, will always be less than the loading shown in Figure 5, and the depth of the shafts can be reduced accordingly. The corresponding shaft depth as functions of slide depth and panel horizontal length per shaft are shown in Figures 6 and 7.

A relationship relating shaft depth as a function of wall height and level of distributed lateral load was determined for the following cost analysis. This relationship is used to determine the depth of shafts where the loading on the shaft is limited by the moment-carrying capacity of the wall panels. This relationship was developed using the multiple regression analysis feature of Lotus 1-2-3. For an 18-in. drilled shaft, the total depth of shaft (L), including the length of the supporting section behind the wall, is

$$L(\text{in.}) = 93 + 10.58\,D(\text{ft}) + 0.1451\,P(\text{lb/in.}) \quad (3)$$

For 24-in. shafts, the total shaft depth is

$$L(\text{in.}) = 130.9 + 9.87\,D(\text{ft}) + 0.1265\,P(\text{lb/in.}) \quad (4)$$

where D is the depth of slide in feet (assumed equal to the height of wall) and P is the resulting wall loading per unit length over the loaded section. Equations 3 and 4 are accurate to plus or minus 8 in. However, when the conservative assumption of an earth pressure coefficient of unity is considered, Equations 3 and 4 can be used with little error.

The two shafts at the ends of the wall carry one-half of the load of the interior shafts. When the depths of the two end shafts are estimated, they are usually found to be within about 2 ft of the depth of the interior shafts.

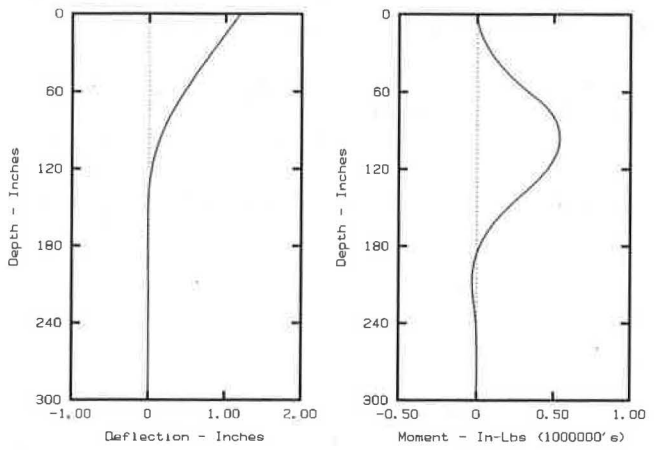

FIGURE 4 Eighteen-in. shafts supporting 5-ft-high wall.

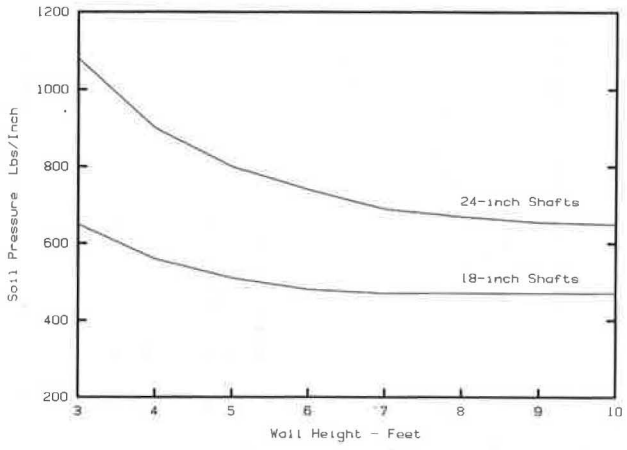

FIGURE 5 Allowable soil pressures acting on wall.

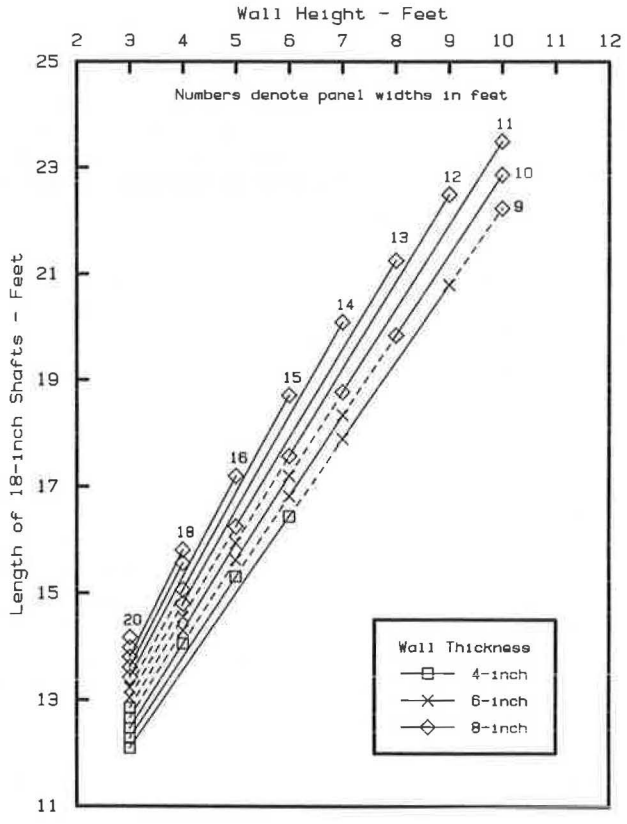

FIGURE 6 Design chart for 18-in. shafts.

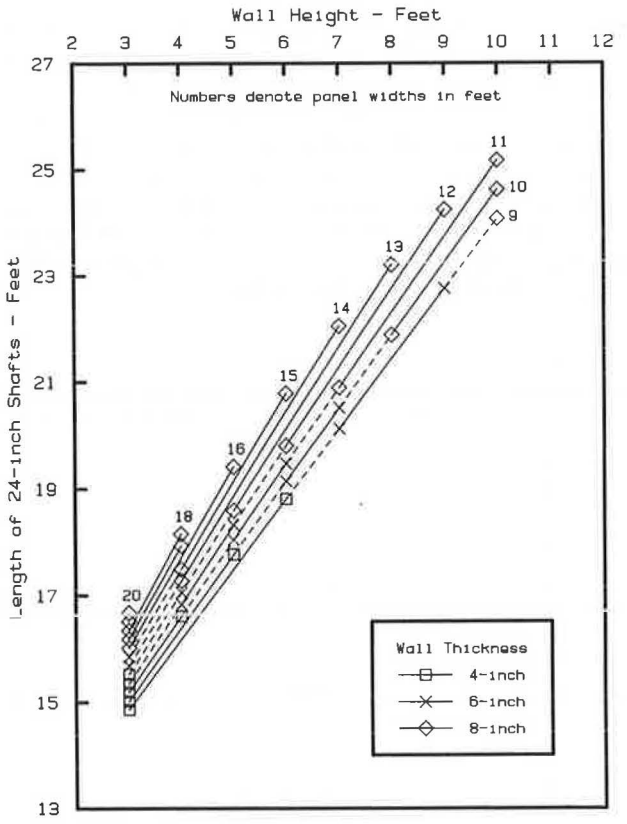

FIGURE 7 Design chart for 24-in. shafts.

COST ANALYSIS

Description of Procedure

The procedure used to evaluate the most economical layout for the drilled shafts and wall slabs for a given wall height is the following:

1. Figure 6 or Figure 7 is consulted to select a slab length and shaft depth.
2. Table 3, Table 4, or Table 5 is consulted to select the appropriate wall slab.
3. The cost per unit area of the wall is evaluated from the total costs of drilled shafts plus wall panels divided by the total area of the wall.
4. The first three steps are repeated for various lengths of slab and the unit costs of wall are compared.
5. The arrangement with the lowest unit cost is selected.

This procedure allows the designer to adjust the final details of the design to reflect the costs of the separate components in a slide suppressor wall. For example, costs of drilled shafts vary by location. As a result, in some areas, walls using a smaller number of longer shafts may be more economical than walls using a larger number of shorter shafts. Another source of variation is the relative cost of various diameters of shafts to carry a given lateral loading. In general, the cost of a slide suppressor wall is largely determined by the cost of the drilled shafts used to support the wall, with the cost of the slabs having a secondary influence.

Ranges for Unit Costs

In Texas, the costs of drilled shafts and precast concrete slabs are calculated on a per-unit-length basis. As an example, the average costs of drilled shafts are \$24/ft for 18-in. drilled shafts and \$45/ft for 24-in. drilled shafts. The unit prices for the precast concrete slabs are also quoted by the linear foot, but usually average about \$200/yd^3 in cost when calculated on a per-unit-volume basis. By using the cubic yard figure, the designer can rapidly estimate the costs for 4-in., 6-in., and 8-in. slabs of various lengths and heights. The above figures were used to calculate the unit costs for walls supported by 18- and 24-in. drilled shafts. These costs are shown in Tables 7 and 8.

The unit costs shown in these tables compare favorably with unit costs for conventional retaining structures. Walls sup-

TABLE 7 COST AND SIZE INFORMATION FOR WALL SUPPORTED BY 18-IN. SHAFTS

Wall Height feet	Shaft Spacing ft	Shaft Length ft	Wall Thickness inches	Unit Cost \$/ft^2
3	13	13.0	4	\$10.47
4	18	16.0	8	\$10.27
5	10	15.5	4	\$9.91
6	9	16.5	4	\$9.80
7	14	20.5	8	\$9.96
8	13	21.5	8	\$9.90
9	9	21.0	6	\$9.93
10	11	23.5	8	\$10.07

TABLE 8 COST AND SIZE INFORMATION FOR WALL SUPPORTED BY 24-IN. SHAFTS

Wall Height feet	Shaft Spacing ft	Shaft Length ft	Wall Thickness inches	Unit Cost $/ft²
3	20	17.0	8	$17.69
4	18	18.5	8	$16.50
5	16	19.5	8	$15.91
6	15	21.0	8	$15.44
7	14	22.5	8	$15.27
8	13	23.5	8	$15.11
9	12	24.5	8	$15.15
10	11	25.5	8	$15.37

ported by 18-in. drilled shafts ranged in cost from $9.80/ft² to $10.47/ft², and walls supported by 24-in. drilled shafts ranged from $15.11/ft² to $17.69/ft² for this example. Cantilever retaining walls often cost about $30/ft² to $35/ft². Mechanically stabilized earth walls typically cost about $25/ft² to $30/ft². Crib-lock retaining walls cost about $12/ft² to $15/ft². In consideration of these costs, slide suppressor walls can be a practical alternative to conventional retaining structures.

CONSTRUCTION CONSIDERATIONS

Slide suppressor walls are practical in areas where right-of-way is restricted and the slide surface is not deep-seated. As a result, the designer should be aware of possible restrictions on construction. Restrictions commonly encountered are restricted access to the site and clearance problems with overhead electric lines. Other considerations are the lifting stresses in the wall panels during placement and orientation so that the panels are facing the correct direction. These restrictions should be considered and proper guidance should be given contractors as necessary.

A second consideration is the stability of the shallow soils above the wall. During construction of the wall, two precautions can be taken to improve the stability of the shallow soils above the wall. First, by providing a drain on the up-hill side of the wall—using a geocomposite drain or backfilling around the wall with a freely-draining soil—the pore pressures in saturated soils can be reduced. A second precaution is to replace the surficial soils with soil of lower plasticity. Soil of this type is less susceptible to the effects of weathering than the highly plastic clays.

A third consideration is corrosion protection of the ends of the prestressing cables in the wall panels. It is common to cast several solid flat slab panels end-to-end on a casting table and then saw the individual panels apart after the concrete has set. This process leaves the prestressing strands exposed and subject to corrosion. Precautions should be taken to protect the exposed strands. One method is to place an expanded foam spacer around the prestressing strand at the location of the saw cut before concrete is placed. After the saw cut has been made, the spacer is removed, any excess strand is cut off, and the remaining void is filled with epoxy cement.

Finally, the designer should consider the magnitude of the bearing stresses on the wall panel at the point of support. If bearing stresses are excessive, a bearing pad should be included in the design.

SUMMARY

Slide suppressor walls can be used to repair slope failures in areas where right-of-way is limited. The procedure developed by the Texas State Department of Highways and Public Transportation for design of slide suppressor walls was presented. This design procedure was based on a simplified method of calculating earth pressures acting on a wall embedded in a slope that has failed and was developed considering the behavior of the supporting drilled shafts and the load-carrying capacity of standardized prestressed flat slabs. The required depths of 18-in. and 24-in. drilled shafts to support wall panels of various lengths are summarized in Figures 6 and 7, and the reinforcing strand pattern designations for 4-, 6-, and 8-in.-thick walls are summarized in Tables 3, 4, and 5. An analysis of the estimated costs found that slide suppressor walls can be cheaper to build than conventional retaining structures.

ACKNOWLEDGMENT

The authors want to recognize Bobby L. Myers, District Engineer of SDHPT District 1, Paris, Texas, for his encouragement of the work documented in this paper.

REFERENCES

1. T. G. Abrams, and S. G. Wright. *A Survey of Earth Slope Failures and Remedial Measures in Texas*, Research Report 161-1, Project 3-8-71-161, Center for Highway Research, The University of Texas at Austin, 1972.
2. P. A. Stauffer, and S. G. Wright. *An Examination of Earth Slope Failures in Texas*. Research Report 353–3F, Project 3-8-83-353, Center for Transportation Research, The University of Texas at Austin, 1984.
3. *PCI Design Handbook*. Prestressed Concrete Institute, Chicago, 1985.
4. S. T. Wang, and L. C. Reese. *Documentation of Computer Program STIFF1*. Ensoft, Inc., Austin, Tex., 1987.
5. L. C. Reese. *Documentation of Computer Program LPILE1*. Ensoft, Inc., Austin, Tex., 1985.
6. H. Matlock. Correlations for Design of Laterally Loaded Piles in Soft Clay. *Proc., 2nd Annual Offshore Technology Conference*, Houston, 1970, Vol. 1, pp 577–594.
7. B. B. Broms. Lateral Resistance of Piles in Cohesive Soil. *Journal of the Soil Mechanics and Foundations Division*, ASCE, Vol. 90, No. SM2, Mar., 1964, pp. 27–63.

TER-VOILE Retaining Works

VALERIAN CURT

The TER-VOILE concept is a process for building retaining walls. A thin shell structure provides stability through the high level of interdependence between the mass to be retained and the structural elements. The basic structural element is the thin membrane. It is a spatial, U-shaped cell that opens towards the backfill. This unit can be made from curved or straight corrugated steel sheet, mesh, or from a sheet-mesh combination. The combination of several membranes and their backfill constitutes the retaining wall. The formation of arches on the horizontal plane within the membrane creates the soil-structure interdependence that makes the TER-VOILE structure a single monolithic mass.

The TER-VOILE® process is used to create structural units that are satisfactorily able to resist vertical and horizontal pressures. This resistance is achieved through the high level of interdependence between the cellular structure formed by the thin, factory-produced membrane and the large volume of earth on the site. The earth-structure combination results in a monolithic composite mass, similar to concrete gravity walls.

The basic structural element is a thin membrane (the "voile") which is designed to produce a U-shaped cell opening towards the backfill. The TER-VOILE structure uses materials of adequate tensile strength.

Figures 1 and 2 show a TER-VOILE cell with its characteristically curved central portion (the "facing") and the two straight end edges (the "restraints"). The basic cell is made of sheet metal or mesh, or of a sheet-mesh combination.

The U-shaped membranes are placed side by side as shown in Figure 3 to form the TER-VOILE structure. Successive layers of backfill (soil) inside the cells ensure interdependence between the structure and backfill, thus completing the soil-cell structure (Figure 4). The TER-VOILE structure is subject to constant tension and utilizes the mechanical properties of the construction materials to the fullest extent.

The thin membrane structure is specially selected and custom made. The backfill is taken directly from the construction site. This backfill is generally good-quality granular materials from borrow pits and already used in construction. In certain cases, laboratory testing may be required. In practice, construction will be facilitated by taking at least 2 m for the width of each cell. Assembly may then proceed by bolting together the face plates and the restraints (or anchors).

This description is based on classical soil mechanics as applied to TER-VOILE structures, supported by tests on numerous scale models (*1*,*2*) as well as by observations on the structures at University of Sherbrooke and Grandes Piles (*2*). However, the description does not enter into the special anchoring required for wire-mesh TER-VOILE structures.

TER-VOILE, Inc. 45 Avenue de Bercy, Candiac, Quebec, Canada J5R 4B8.

In short, TER-VOILE creates composite structural units based on the interdependence between the structure and the mass to be retained. Backfilling completes the procedures.

THEORETICAL BASES

Cell Geometry

For this study of a retaining device, a basic unit will be examined consisting of a cell formed by a facing, two restraints, and a reference plane (fictional) (Figure 5). The system of coordinate axes and geometric characteristics are also shown in this figure.

Earth Pressure

Earth pressures are important factors in the calculation of TER-VOILE retaining structures. The effect of these forces is derived from well-known theories that are widely documented (*3*,*4*).

With regard to TER-VOILE structural units, earth pressures are considered to be applied within the structural cell—on the facing and restraints in particular. The TER-VOILE cell, with backfill confined to the inside of the cell, is then subject to earth pressures on the structural cell coincident with the back of the restraints.

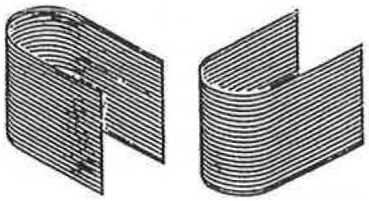

FIGURE 1 Thin shell (plate).

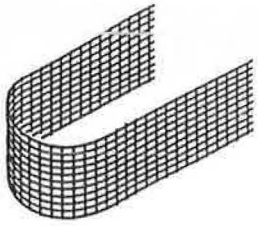

FIGURE 2 Thin shell (wire mesh).

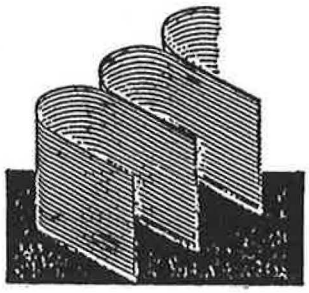

FIGURE 3 TER-VOILE cells.

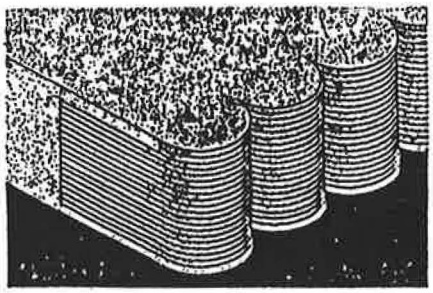

FIGURE 4 TER-VOILE structure.

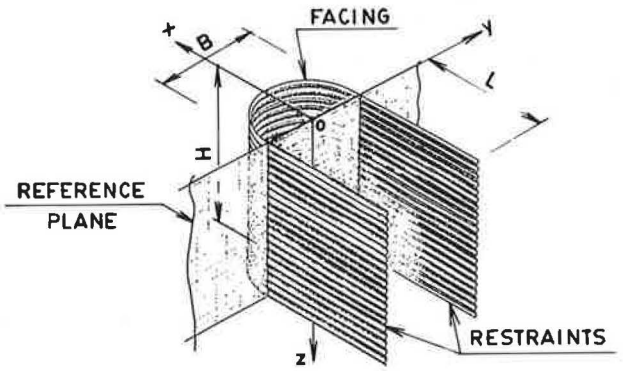

FIGURE 5 TER-VOILE geometry.

DIMENSIONING

The TER-VOILE structure must be designed to ensure (a) resistance to the worst combination of exterior pressures and (b) behavior as an integral unit of earth and thin element. Overall stability must be ensured as for any gravity structure.

Internal Stability

The TER-VOILE structure shown in Figure 6a is considered to be subject to earth pressures on the reference plane (Figure 6b). Similarly, earth pressures are exerted within the unit on the restraints (Figure 6c). It should be noted that according to measurements (*5*) earth pressures exerted on the reference plane are compatible with the (constant) coefficient of pressure at rest. At the current stage, the use of a constant K_o is proposed by the author.

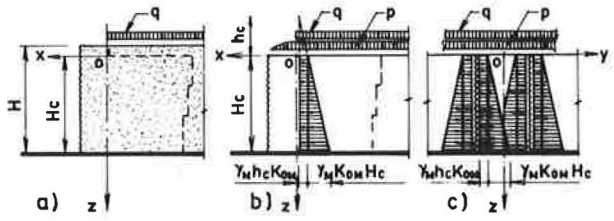

FIGURE 6 Thrust from inside a cell.

Consequently, stresses within the TER-VOILE structure at depth z are as follows:

1. The vertical unit stress (a function of depth, z):

$$\sigma_z = \Phi(z) \tag{1}$$

and

2. The horizontal unit stress in all directions:

$$\sigma_x = \sigma_y = K_o \sigma_z \tag{2}$$

K_o is the at-rest pressure coefficient, which is calculated as

$$K_o = 1 - \sin \phi \tag{3}$$

where ϕ is the internal angle of friction of the backfill.

Unit stresses in the thin membrane of the TER-VOILE cell are determined using the following methodology (Figure 7):

Step One

The semicircular facing used in this example may be compared to a cylindrical shell whose reference plane coincides with a diameter.

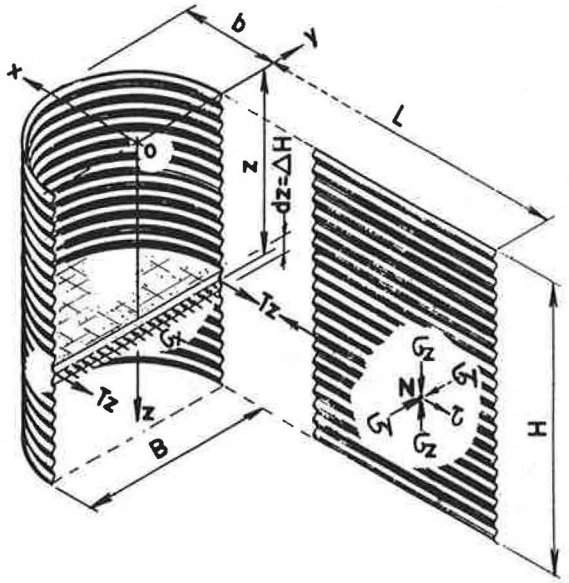

FIGURE 7 Forces on structure.

The cylindrical facing shell is very thin compared to the radius of curvature. Consequently, the stresses can be calculated with high precision by assuming that tensile stresses are uniformly distributed across the thickness of the shell.

The half cylinder that forms the facing and is subject to earth pressure may also be considered to be a very long, thin-walled cylindrical reservoir. Its tensile stress can be calculated for a unit with height ΔH at depth z as the following transmitted to the restraints:

$$\tau_z = \frac{1}{2}\sigma_x \cdot B \cdot \Delta H \tag{4}$$

The restraints are acted on by two contiguous facings.

Step Two

The internal angle of friction ϕ is a characteristic of the backfill. The soil-structure angle of friction ψ depends on the surface of contact. From the observations on scale models (*5*) and the structures already built, this angle is relatively high. This high angle results from the creation of arches (discussion to follow). With current knowledge, the design criteria (*6*) used do not allow for an angle ψ in excess of 75 percent of the angle ϕ.

However, by using high-adherence (embossed) surfaces for soil-structure contact, ψ may be taken equal to ϕ, and this assumption will be made in what follows.

The coefficient of friction may be written as

$$f = \tan \psi \leqq \tan \phi \tag{5}$$

The stresses on the restraint plane at a point N are shown in Figure 7.

The values of σ_x, σ_y and σ_z are given in Equations 1 and 2.

To determine unit tangential stress, Coulomb's linear law for noncohesive materials has been taken:

$$\tau = \sigma_y \tan \phi \tag{6}$$

Given that the restraints may be thought of as an extension of the facing elements, they must be capable of transmitting force into the backfill mass by friction or by shearing. It must be ensured that friction exists without sliding at every point of contact between the structure and the soil. This results in the following equation:

$$f = \tan \phi = \frac{\tau}{\sigma_y} \tag{7}$$

Using Equation 4 and referring to Figure 7, we can see that the tensile stress in the facing is transmitted to the restraints and must equal the sum of the tangential stresses. To express this, point N (Figure 7) will be isolated as a fragment of surface $dl \cdot \Delta H$, as shown in Figure 8. Integration of the equilibrium equation along the restraint gives the required length of the restraint:

$$l = \frac{Tz}{f \cdot \Delta H \cdot \sigma_Y} = \frac{B}{2f} \tag{8}$$

In practice, a factor of safety must be added to this equation, depending on circumstances (*6*). This should be at least 1.5 at every level as well as overall.

A very important feature of the TER-VOILE structure is the formation of arches in the horizontal plane. This is the key factor in the soil-structure interaction that ensures the entire block will function as a unit. Consider a horizontal plane at a certain depth within the TER-VOILE structure. The interaction between the soil and the structure is illustrated in Figure 9.

Earth pressure in both directions is represented by σ_x and σ_y. The stresses σ_y cancel each other, whereas the stresses σ_x tend to destabilize the structure (Figure 9a). To achieve equilibrium, displacement of the structure will result in friction τ (Figure 9b), which counteracts and cancels σ_x. In addition, the sum of stresses $\bar{\sigma}_y + \bar{\tau}$ represents the reactions of the horizontal arches in the backfill. The same action occurs in silos, but in a vertical plane.

The formation of arches is the basis of the monolithic character of the structure and the backfill mass. In TER-VOILE structures, the creation of arches has been proven in laboratory tests on scale models and on the Grandes Piles prototype.

Numerous laboratory tests are available for analyzing the monolithic nature of TER-VOILE cells. Failure has been found to occur when the ratio of restraint length to wall height (L/H) is less than 0.3. With an L/H ratio of 0.4 or greater, deformations are tiny (see Figure 10).

Based on current knowledge, the following formula for calculating dimensions is proposed:

$$L_m = (0.6 \text{ to } 0.7)H_c \text{ with } B \leqq 0.5H_c \tag{9}$$

and

$$L_m \geqq 1.2B > \text{with } B > 0.5H_c \tag{10}$$

The restraints of the experimental structure at Sherbrooke (each cell was 5.5 m high and 2.5 m wide) were fitted with

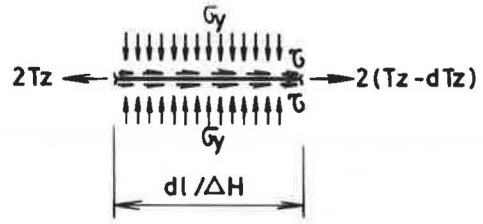

FIGURE 8 Equilibrium of a restraint.

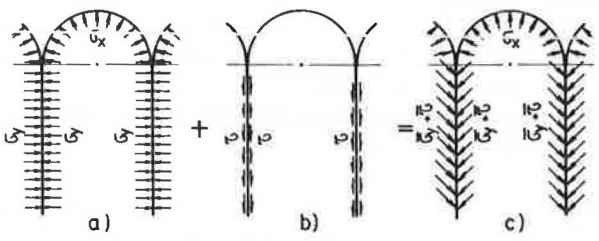

FIGURE 9 Soil-structure interaction.

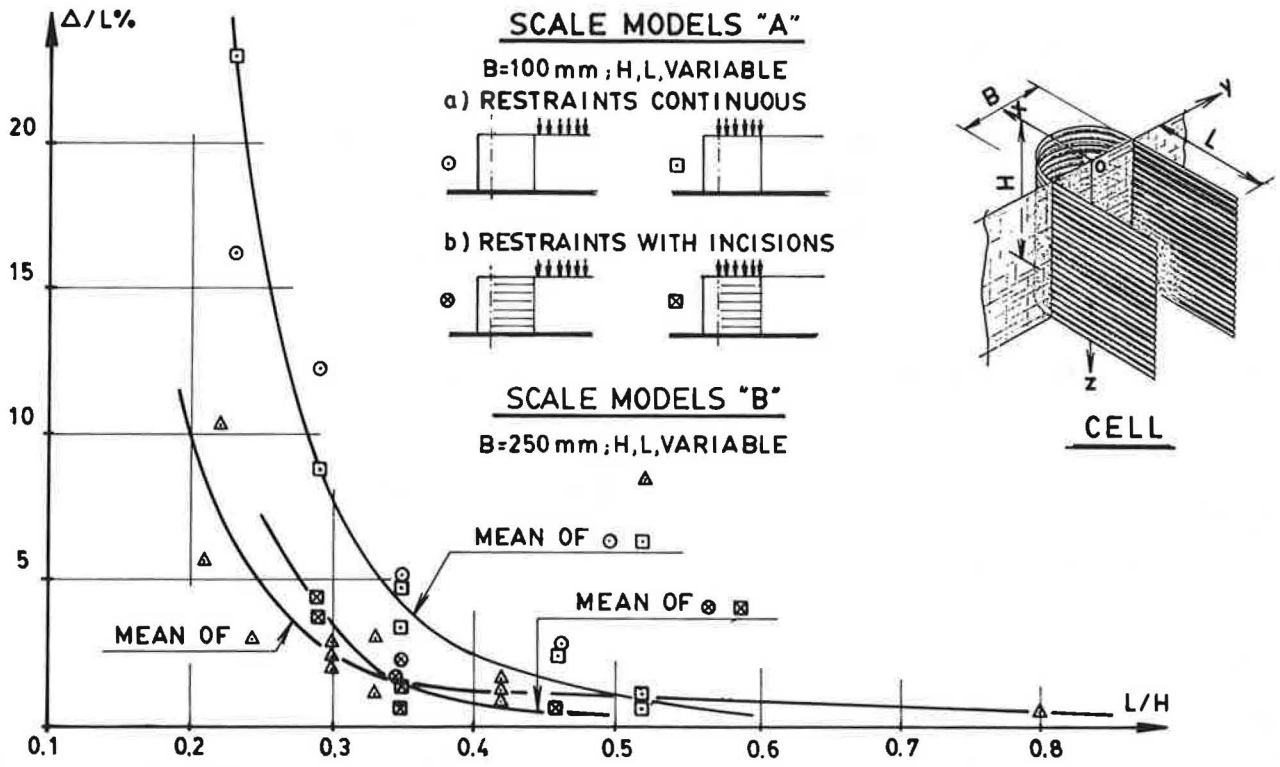

FIGURE 10 TER-VOILE scale models.

dozens of strain gages. The measurements made did not enable a curve of maximum tensile stresses to be drawn.

The extensometers installed in the Grandes Piles structure showed monolithic behavior (no differential movement within the cells (see Figure 11). However, the same tests proved that relative motion did occur with respect to the rear of the unit.

In view of this, the hypothesis of a failed surface, in accordance with classical theory or even in the case of reinforced earth, has been rejected. In a TER-VOILE unit, loss of internal stability may result from (a) structural rupture, (b) the loss of frictional force between backfill and restraints, or (c) the destruction of the arches within the backfill.

The author assumes the destruction of the monolithic nature of the unit as a working hypothesis. This may occur as a possible rupture in the reference plane where facing and restraints are joined—the assembly section being weakest. Between restraints, the surface of rupture should be located near the plane of reference.

In the present state of knowledge, the mechanism whereby the monolithic nature of the unit is destroyed is unknown. Laboratory tests are required to clarify this.

For a complete unit, a curved potential rupture surface is assumed in the interim. This is supposed to pass through point G_o (the centroid of the semicircular facing) at the base, and through point A_o at the upper surface. Practically speaking, the inclined plane through O_{Hc} and A_o may be substituted. This is located everywhere on the right side of the reference plane (Figure 11). In the limit, it will coincide with the reference plane in the case of cells of low height compared with their width.

Equations 9 and 10 are used to find point A_o, with L_m equal to L_z when $z = 0.5H_c$. In this case the surface subject to friction, which should be equal and opposite to the thrust from backfill, is equal to $l \cdot H_c$.

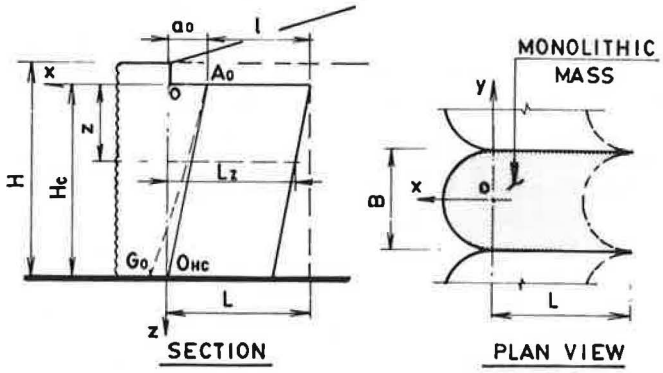

FIGURE 11 Analysis of internal stability.

External Stability

Similar to a concrete gravity wall, the TER-VOILE structure is considered to be acted on by pressure from behind the structure (Figure 12) with a live load from above increased by 50 percent.

For practical purposes, a parallelepiped with rectangle $ABCD$ as its base and height H (Figure 12) may be taken as the stabilizing mass.

Note that distance C_1 defining the plane AB is given by

$$C_1 \cdot B = 1/8\ \pi\ B^2 \qquad (11)$$

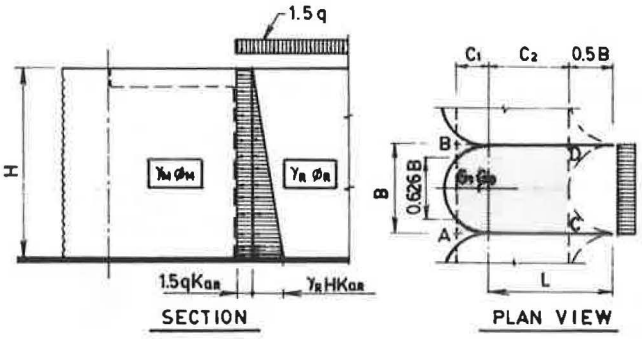

FIGURE 12 Analysis of external stability.

External stability is expressed via the following two equations:

Equation 12 shows stability against overturning:

$$F_r = \frac{M_s}{M_r} \tag{12}$$

where

F_r = factor of safety against overturning,
M_s = stability moment, and
M_r = overturning moment.

In overturning, there must be an axis of rotation of the TER-VOILE cell at foundation level. The precise position of this axis is unknown. The plane of reference is too conservative and the front of the semicircular facing is not realistic. The author suggests an axis of rotation located between G_o (centroid of the semicircle) and G_1 (G_1 is on the line AB) (see Figure 12).

For these reasons, the factor of safety against overturning F_r should be 1.5 with respect to an axis passing through G_o, and 2.0 with respect to one through AB.

Equation 13 shows stability against sliding at the base:

$$F_g = \frac{W}{P} \tan \phi_1 \tag{13}$$

where

F_g = factor of safety against sliding,
W = weight of entire retaining structure,
P = earth pressure, and
ϕ_1 = internal friction angle of foundation soil.

In practice, we suggest a factor of safety against sliding of at least 1.5.

FOUNDATION AND BACKFILL

The site where a retaining wall is to be erected is never a free choice. Similarly, the foundation soil comes part and parcel with the site and must be accepted with all its shortcomings as well as its positive qualities.

The high structural elasticity of TER-VOILE retaining walls makes them adaptable to very poor foundation conditions. In fact, when the terrain is uniform, is relatively unaffected by water, demonstrates great strength, and has good drainage, retaining walls do not even require a special foundation.

In the construction of retaining walls, two types of backfill must be distinguished. The first, in-cell backfill material, is placed within the cell and provides the necessary structural interdependence with the membranes. Its physical characteristics (Figure 12) are identified as γ_M and ϕ_M.

The second is rear backfill material. The space between the wall and the natural ground slope can be filled using the same material as that used within the cells or with another material of poorer quality. This type of backfill will exert pressure on the in-cell backfill and may produce external instability of the structure. Rear backfill is identified in Figure 12 by γ_R and ϕ_R.

DURABILITY OF STRUCTURAL MATERIALS

As previously stated, the structural element is a thin membrane (the "voile"). Because this membrane is manufactured, its characteristics can be selected as needed. The material used to make the membrane must have high tensile strength and meet architectural and environmental requirements. In addition, the materials used and their coatings must be selected according to the nature of the backfill.

The main materials suitable for the manufacture of TER-VOILE structural elements are

- Galvanized or nongalvanized steel,
- Stainless steel,
- Cor-ten steel,
- Steel alloys,
- Aluminum alloys, and
- Composite plastic materials.

The most widely used material for retaining structures is mild steel in the form of galvanized or nongalvanized, corrugated sheet metal (or mesh), or aluminum alloys. Aluminum alloys should be of the type used for piping or piles. Aluminum alloys need careful attention, depending on the nature of the soil.

If, for better appearance, stainless or cor-ten steel is selected for the facing, galvanized steel may be used for the restraints. For example, stainless steel behaves poorly when it comes in contact with certain types of soil. On the other hand, the behavior of cor-ten steel in contact with soil is not well documented. Generally speaking, direct contact between both types of steel and soil is to be avoided. Bituminous coatings with polymers or the equivalent may be used.

Among other steel alloys, the best results have come from steel containing copper. This alloy has excellent fresh water resistance. Composite plastic will be an option in the future.

The structural elements forming the cell may be either a continuous membrane or a wire mesh used alone or in combination with poured concrete or gunite. Small precast concrete blocks can be combined in a variety of ways with the facing. Precast concrete panels can be used for the facings.

The useful life of these retaining walls varies. The durability of the structural elements depends on the resistance to corrosion of the materials used. The rate of corrosion is closely linked to the compatibility between these materials and the surrounding environment, particularly the characteristics of the backfill soil.

The chemical and electrochemical characteristics of the foundation soil, along with the in-cell backfill, determine the degree of corrosion. In practice, it is possible to limit corrosion of structural metal by choosing appropriate backfill material. It is impossible to totally eliminate corrosion; however, it can be limited to within a tolerable range.

Protection against corrosion is closely related to the electrochemical nature of the deterioration process. The main types of protection are

- Coatings,
- Cathodic protection, and
- Additional thicknesses.

TER-VOILE STRUCTURES

Usual Structures

The basic TER-VOILE structure was discussed earlier in this paper (Figures 1 and 2). For reasons of aesthetics, strength, or durability, the structure may include a façade covering, such as injected concrete (gunite) (Figure 13).

If a relatively thick gunite coating is desired, the use of mesh is recommended. As shown in Figure 14, the mesh may be attached to the restraints, which are extended specifically for this purpose. This means that a very thin metal sheet (capable of withstanding earth pressures during construction) may be used as a facing. However, the mesh must be sized to take the full extent of earth pressures.

Structures with Joined Facings

A structure with joined facings or "junctions" combines the basic structure with the U-shaped elements joined at the façade by convex elements (Figure 15).

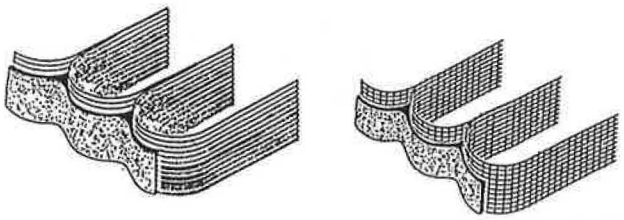

FIGURE 13 Gunited structure: overall view.

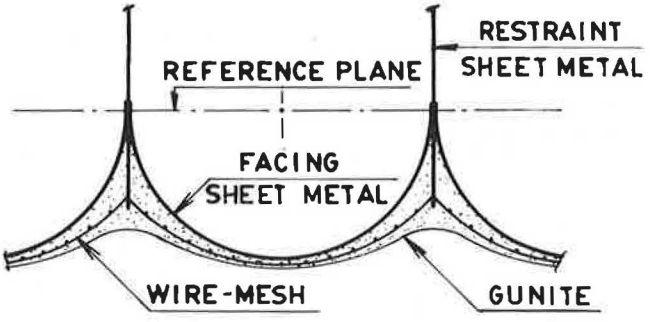

FIGURE 14 Gunited structure: plan view.

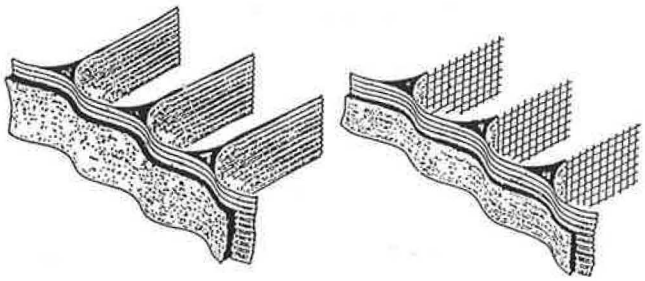

FIGURE 15 Gunited junction-type structure: overall view.

The façade may be covered or bare. Figure 16 shows a plan view of the detail of a junction type structure. This structure has recesses that may be filled with concrete or reinforced concrete. This is a particular advantage for bridge abutments.

Coated Structures

These structures are specially designed so that a coating can be attached to the facing. The facings of these structures are circular arcs with a camber between one-third and one-half of the radius (Figure 17).

The facings and restraints are hooked together bar by bar or by using rods.

The structures shown in Figure 17 can be backfilled "as is" if rock fill is used, or by installing a membrane between the backfill and the mesh facing. The membrane, acting as a liner, prevents the passage of materials through the facing. It can be made of metal or plastic sheet or a thick geotextile.

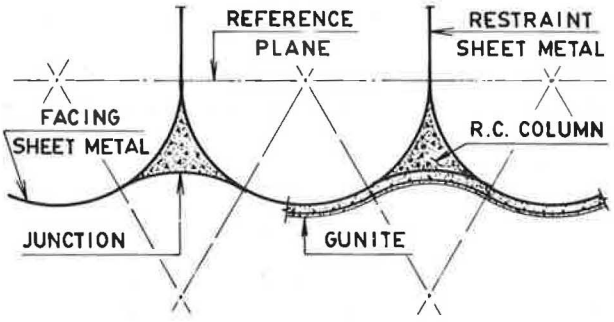

FIGURE 16 Gunited junction-type structure: plan view.

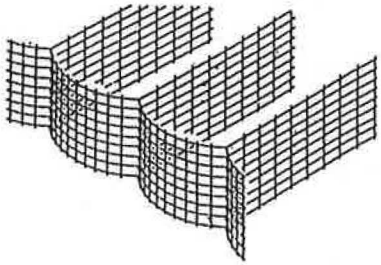

FIGURE 17 Wire-mesh structure: overall view.

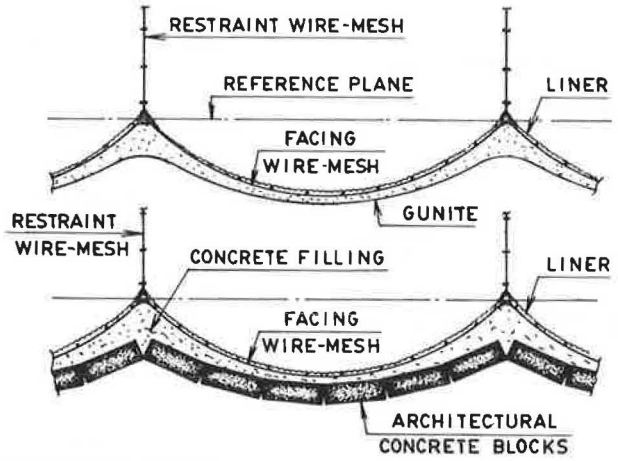

FIGURE 18 Coated wire-mesh structures.

Figure 18 shows this covering first with gunite and secondly with architectural concrete blocks.

CONCLUSIONS

It is hoped that the TER-VOILE concept will take its place among retaining wall designs that foster interdependence between structure and backfill.

The existence of such types of structure may be traced back to the dawn of civilization. Several writers have described armored earth structures and armored earth structural components used in ancient times or even by animals (*7*).

The old principles have recently been revitalized and optimized. Soil friction has been known from time immemorial; however, with the wide acceptance of armored earth, it has never been studied and tested with such persistence as nowadays.

From this standpoint, REINFORCED EARTH has succeeded in greatly advancing the knowledge of soil friction with masterly use of this ancient principle. REINFORCED EARTH has been a great revelation in its time.

Cribs used for retaining walls are also very ancient. In antiquity wood was used; steel and concrete have appeared too in modern-day construction. Several types of crib walls using corrugated galvanized steel or aluminum alloys have been developed, particularly those built from complete pipe sections or small bore pipes slit along a diameter.

TER-VOILE uses the age-old principle of cribs and optimizes to the utmost. The basic TER-VOILE cell described in this article is a structure subject to tension only; the author takes the liberty of claiming this to be a novelty.

Arching in backfill has also been known since time immemorial and has been studied in great detail in silos, but much less attention has been given to its use in retaining walls. TER-VOILE cells, with their reliance on soil friction, highlight the formation of arches in the horizontal plane.

Though not revolutionary, TER-VOILE is a step forward in optimizing retaining structures and has novel features. It is a new principle, then, and not to be confused with its established peers.

GLOSSARY

ox, oy, oz	=	axes of coordinates
H	=	overall length of structure
H_C	=	height for computation
h_c	=	equivalent height of extra loads (live and dead)
B	=	width of cell
b	=	camber of facing
L	=	overall length of restraints
L_z	=	length of plane of restraints at depth z
L_m	=	average length of plane of restraints
l	=	length of restraints for computation
G_o	=	center of gravity of the surface enclosed by facing and reference plane
W	=	weight of entire retaining structure
P	=	earth pressure
F_r	=	factor of safety against overturning
F_g	=	factor of safety against sliding
M_s	=	stability moment
M_r	=	overturning moment
g	=	live load
p	=	dead load
T_z	=	reaction from facing due to thrust from backfill at depth z
ϕ	=	internal friction angle of the backfill
ϕ_1	=	internal friction angle of foundation soil
ϕ_m	=	internal friction angle of backfill
ϕ_r	=	internal friction angle of fill in rear of structure
ψ	=	soil–structure friction angle
f	=	soil–structure friction coefficient
K_o	=	coefficient of pressure at rest
K_{om}	=	coefficient of pressure at rest of backfill
K_{ar}	=	coefficient of active pressure of fill in rear of structure
γ_m	=	specific weight of backfill
γ_r	=	specific weight of fill in rear of structure
Φ	=	function of variable z
G_z	=	stress in vertical direction
G_x	=	stress in horizontal direction
G_y	=	stress in horizontal direction
τ	=	friction stress between soil and restraint
τ_z	=	friction stress between soil and restraint at depth z
$dr = \Delta H$	=	infinitely small element of height

REFERENCES

1. J. P. Morin, and V. Curt. TER-VOILE RETAINING STRUCTURES. Presented at the 12th International Conference on Soil Mechanics and Foundation Engineering, Rio de Janeiro, Aug. 13–18, 1989.
2. V. Curt, et al. Un Noveau Concept de Soutenement, le Procede TER-VOILE. *Annales de l'Institut Technique du Batiment et des Travaux Publics*, No. 454, Paris, France, May 1987.
3. K. Terzaghi. *Theoretical Soil Mechanics*. John Wiley and Sons, Inc., New York, 1943.
4. W. C. Teng. *Foundation Design*. Prentice-Hall Inc., Englewood Cliffs, N.J., 1962.
5. J. P. Morin. *TER-VOILE, Rapport de Recherche*. University of Sherbrooke, Sherbrooke, Quebec, Canada (in press).
6. V. Curt. *Critères de Design TER-VOILE*. Internal Report, Quebec Ministry of Transportation, Quebec, Canada, 1988.
7. C. J. F. P. Jones. *Earth Reinforcement and Soil Structures*. Butterworths, London, 1985.

Dynamic Stability of Soil-Reinforced Walls

JOHN VRYMOED

A method is developed to determine the static and dynamic stability of soil-reinforced walls. The method determines factors of safety against pullout and yield of the reinforcement and against the wall sliding on its base. These factors of safety are determined as a function of different levels of acceleration applied at the base of the wall. Results are shown when the proposed method was used to determine the stability of a 62-ft high wall constructed as part of the realignment of State Highway 101 in northern California.

The California Department of Transportation (Caltrans) has investigated the various aspects of soil-reinforced walls during the past decade subsequent to Vidal's pioneering in this area (*1*). Because of the great potential oif soil-reinforced walls in reducing the cost of transportation-related construction, Caltrans actively promotes their use when site conditions are favorable. The design and construction of these walls is relatively simple and the procedures are now familiar to many in the profession. In California, one of the inevitable facts of building soil-reinforced walls is the high levels of acceleration that need to be considered for the majority of sites. This is why a practical method and guide was sought that would easily determine the adequacy of any given design under both static and dynamic load conditions.

PREVIOUS INVESTIGATIONS

The first known investigation into the behavior of soil-reinforced earth walls under dynamic load conditions was done by Richardson and Lee (*2*) in 1975. In their investigation, small model walls were constructed and subjected to horizontal accelerations generated by a shaking table. The results of these model tests suggested that the tie forces could be defined by a straightline envelope as a function of horizontal acceleration. To obtain this horizontal acceleration, the use of response spectra and modal participation factors was recommended.

Additional shake table tests on small model walls were carried out by Wolfe et al. (*3*) to determine the effect of vertical accelerations on the tie force and wall displacements. It was concluded from the test results, that for walls having low strain frequencies greater than the dominant frequencies of vibration, the effect of the vertical component of acceleration could be ignored.

Richardson et al. (*4*) conducted field studies on a full scale 20-ft-high wall to test and improve the recommended seismic design derived from the earlier model studies. The field studies used mechanical vibrators and explosives to subject the wall to different levels of excitation. The mechanical vibrators were only able to induce relatively low maximum shear strains of less than 0.001 percent. The explosives, however, induced large strains with associated peak accelerations in excess of 0.5 g at the top and bottom of the wall. The strain resulted in a permanent outward movement of 5 percent of wall height. The dynamic tie forces measured during the explosive tests were much less than the forces predicted by the seismic design based on the small model tests. Because of this discrepancy, the seismic design was revised by Richardson (*5*) to reproduce the tie forces observed in the explosive tests. To accomplish this, the modal participation factors for the first and second mode of vibration were reduced from the earlier recommended values.

This revised design procedure was used by McKittrick and Wojciechowski (*6*) in the design of five soil-reinforced walls at Valdez, Alaska. The structures were designed to withstand a magnitude 8.5 earthquake with associated peak spectral accelerations of 0.5 g and 0.71 g for the first and second modes, respectively. The consequence of incorporating the dynamic forces was to increase the density of reinforcement near the top of the walls.

PROPOSED SEISMIC DESIGN

The proposed seismic design is a pseudo-static method of analysis that treats the wall as a rigid block and treats the soil retained behind the wall as a rigid wedge. This method circumvents the need to determine the primary and secondary modes and the associated modal participation factors as proposed by previous investigators.

The analysis described herein determines the factors of safety as a function of horizontally applied accelerations for both the internal and external stability of a given wall design. Having determined this function, Newmark's method (*7*) is then used to estimate permanent wall displacements. If it is determined that the displacements are excessive for a given wall design and site-specific seismic parameters, the design can be revised and checked again. This seismic design methodology is similar to the method developed by Richards and Elms (*8*) for gravity retaining walls.

The displacements computed by the proposed method are considered to occur by sliding at the base of the wall and/or by pullout of the reinforcing elements causing an outward tilting of the wall face. Total collapse of the wall would be predicted if the factors of safety against yield of the elements were to drop below unity.

California Department of Transportation, Office of Transportation Laboratory, 5900 Folsom Boulevard, Sacramento, Calif. 95819.

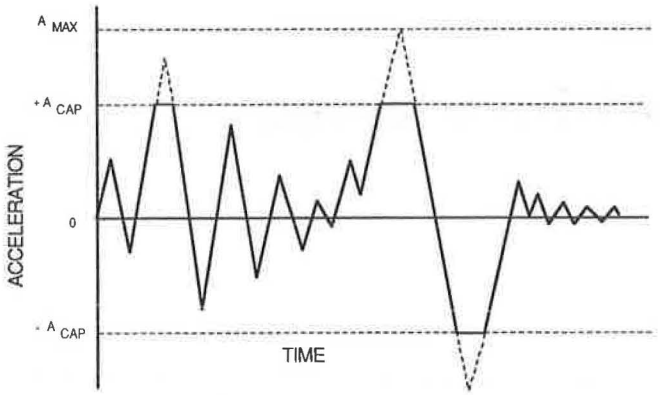

FIGURE 1 Capped acceleration time history.

Because the wall is analyzed for both internal and external stability, the acceleration that a given level of reinforcement experiences may be less than the input acceleration if that acceleration causes sliding to occur at the base of the wall and/or causes the reinforcement below that level to exceed its pullout resistance. Therefore, a given level of reinforcement may experience an acceleration time history which is "capped" as shown in Figure 1. Franklin and Chang (*9*) reported variations of standardized displacements with ratios of critical and peak accelerations. These displacements were computed from acceleration and velocity time histories scaled to peak values of 0.5 g and 30 in./sec, respectively.

Six acceleration time histories were taken and capped at different percentages of peak acceleration to determine the effect of capping on their standardized displacements as shown in Figure 2. Because this figure shows that this effect is negligible, the proposed method uses the relationships developed by Franklin and Chang to estimate standardized displacements when acceleration levels are capped.

EXTERNAL STABILITY ANALYSIS

In the external stability analysis, a soil-reinforced wall supporting a sloping backfill as shown in Figure 3 is considered. The path of the failure plane shown in this figure passes underneath the wall, through the backfill at an angle θ, and then passes vertically until it intercepts the surface of the backfill. The vertical extent of this failure plane is dependent upon the cohesion of the backfill. Although it is common for the embedment lengths to be the same throughout the height of the wall, the angle β shown in Figure 3 allows for the modeling of uniformly changing lengths. The equations derived in this study assume a positive angle β.

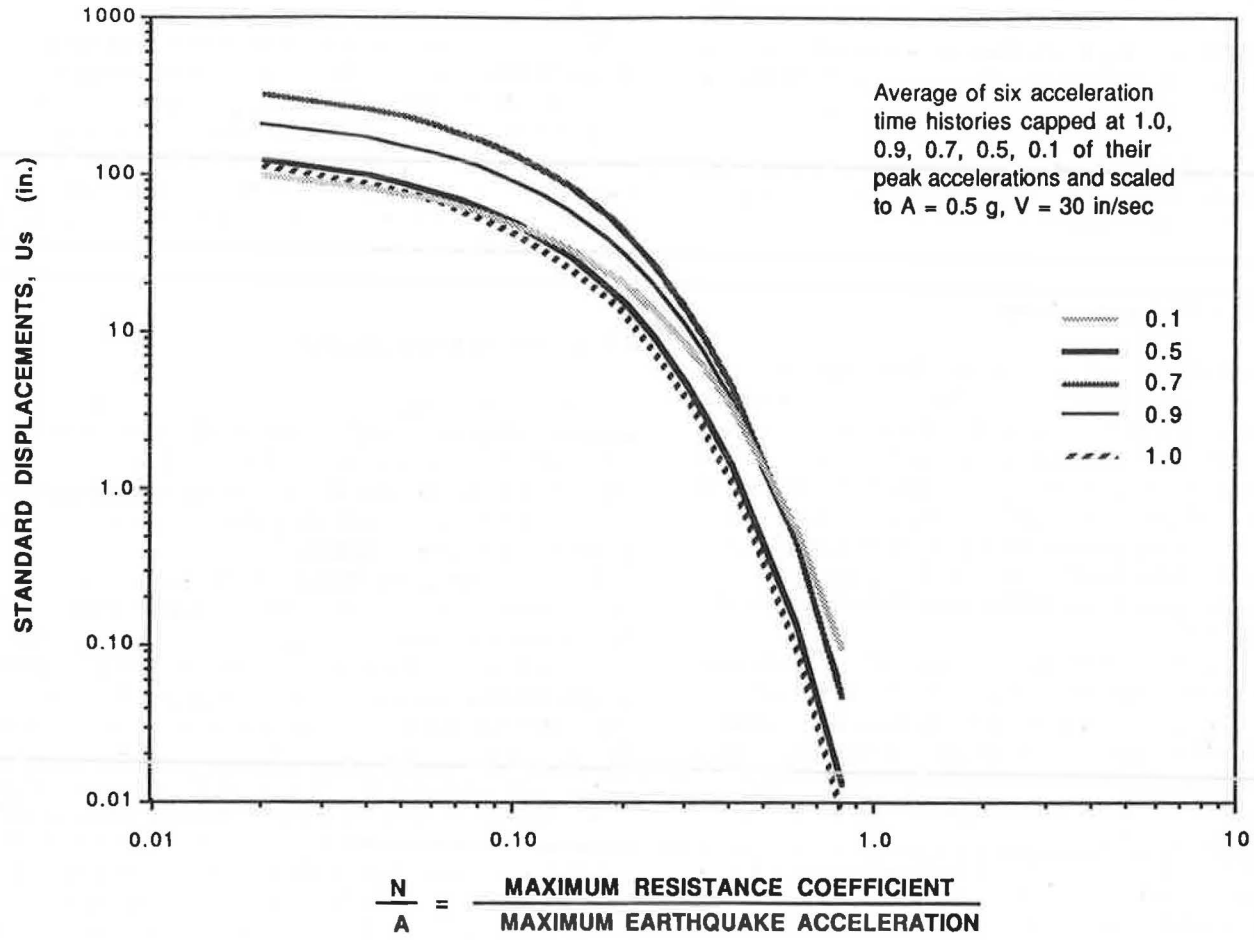

Note: N represents the critical acceleration, which is the acceleration required to reduce the factor of safety to unity.

FIGURE 2 Effect of capping acceleration histories on U_s and values of N/A (*9*).

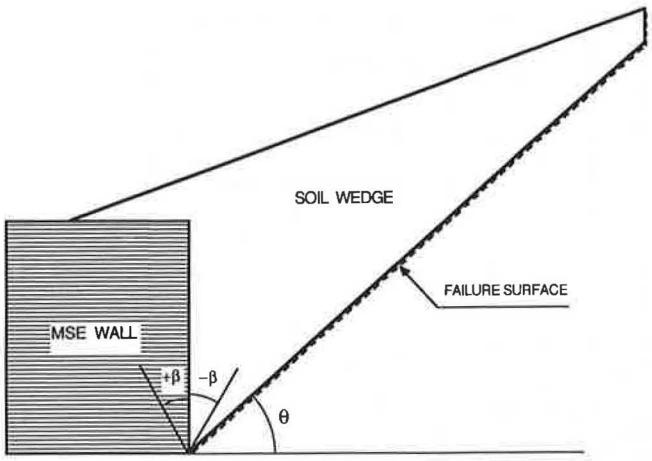

FIGURE 3 External stability analysis of wall and backfill.

A freebody diagram of the wall and the associated forces are shown in Figure 4. In this figure, W_1 represents the weight of the wall including the weight of the sloping backfill directly above it; K_n is the coefficient of acceleration applied in the horizontal direction; C_w and C_a are the forces developed due to cohesion at the wall interfaces; P is the force required for equilibrium of the wedge representing the sloping backfill; N_1 is the resultant force while ϕ_1 and ϕ_2 are the soil's internal friction angles at the wall/foundation and backfill interfaces.

The factor of safety against sliding of the wall, FS_s, is defined by Equation 1.

$$FS_s = \frac{F_r}{F_d} \tag{1}$$

where F_d and F_r represent the driving and resisting forces which are in turn defined as follows:

$$F_d = K_h W_1 + P\cos(\phi_2 + \beta) - C_a \sin\beta \tag{2}$$

$$F_r = C_w + \tan\phi_1 [P\sin(\phi_2 + \beta) + W_1 + C_a\cos\beta] \tag{3}$$

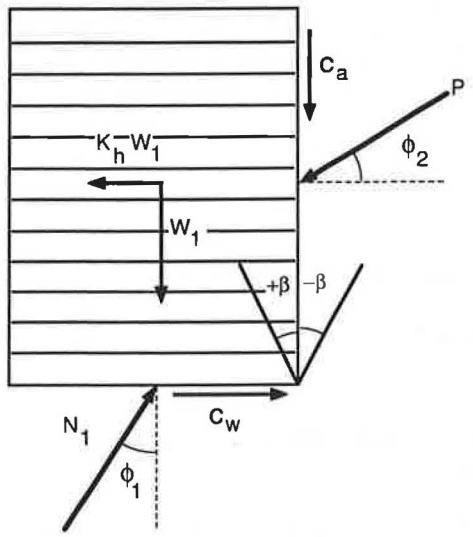

FIGURE 4 Wall freebody and associated forces.

The force P required for equilibrium of the backfill wedge is determined by considering the freebody diagram and the associated forces resolved in a force diagram as shown in Figure 5. In this figure C_L and C_a represent the cohesion forces developed over the lengths shown. The following equation for P is derived by resolving the forces in their horizontal and vertical components and back substituting:

$$P = \frac{B\sin(\theta - \phi_2) - A\cos(\theta - \phi_2)}{\cos(2\phi_2 + \beta - \theta)} \tag{4}$$

where

$$A = C_L\cos\theta - C_a\sin\beta - K_h W_2 \tag{5}$$

$$B = W_2 - C_a\cos\beta - C_L\sin\theta \tag{6}$$

The failure plane's angle of inclination, θ, is varied until the maximum value of P is found. This angle decreases with increasing levels of horizontal acceleration as shown in Figure 6.

The manner in which the external stability of a soil-reinforced wall is determined is similar to the Mononobe-Okabe method (*10,11*) of analyzing the dynamic stability of gravity retaining walls since both are extensions of the Coulomb-Rankine sliding wedge theory. Therefore, comparisons were made between the two methods in terms of $K_{ae}\cos\delta$, which represents the active earth pressure coefficient, and the friction angle of the wall-soil interface. The comparison, shown in Figure 7, indicates that the two methods yield identical results. It should be pointed out that in traditional gravity retaining wall analyses, the friction angle of the wall-soil interface, δ, is taken as one-half of the soil's internal friction angle (i.e., $\phi/2$). In the soil-reinforced wall analysis, the full friction angle is considered at this interface because it is predominantly a soil-to-soil contact. The effect is a reduction in the value of K_{ae} which is also shown in Figure 7.

INTERNAL STABILITY

Assumed Failure Plane

In the internal stability analysis, the factors of safety against yield and pullout of the reinforcement are determined for different levels of horizontal acceleration. In this determina-

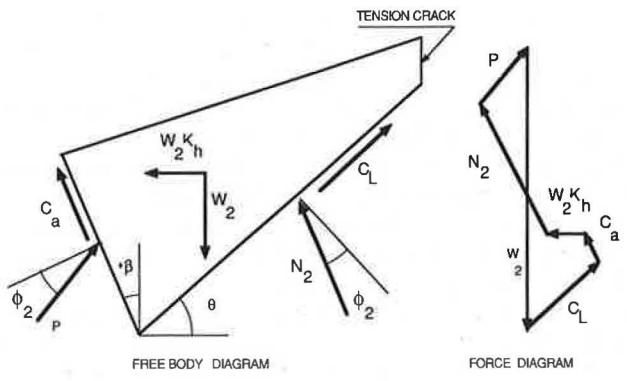

FIGURE 5 Backfill wedge freebody and force diagram.

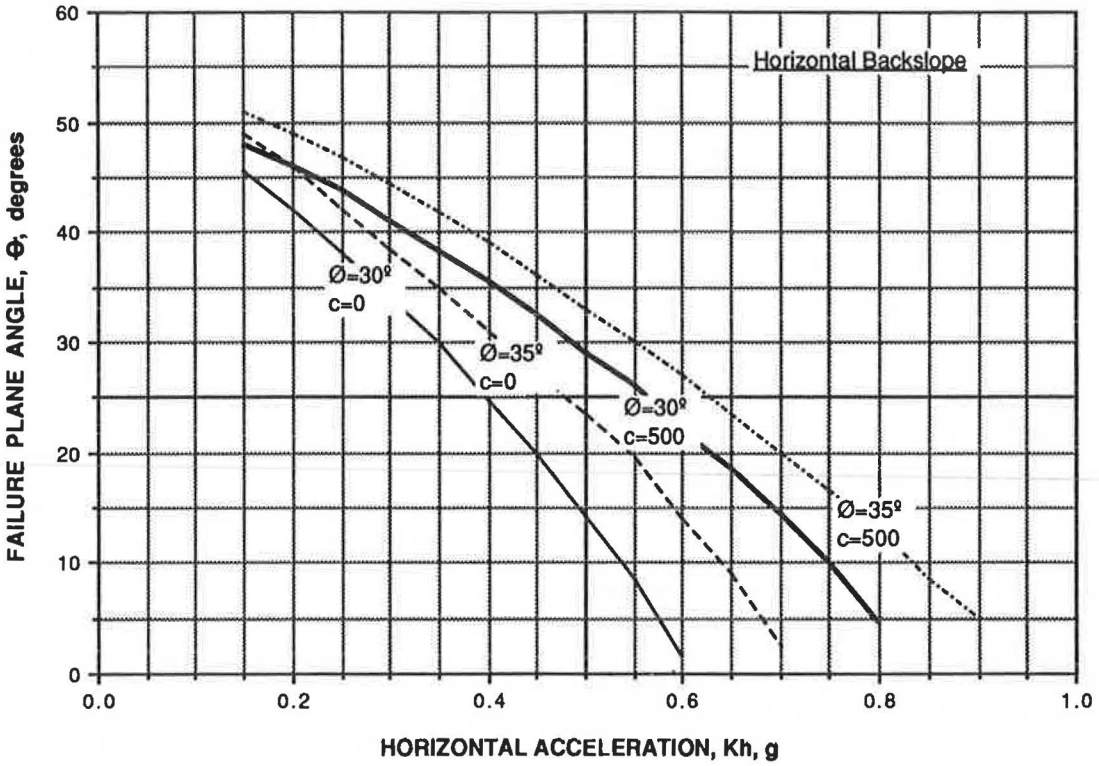

FIGURE 6 Variation of inclination of failure plane with horizontal acceleration.

tion, an assumption has to be made regarding the location and shape of the internal failure plane. Previous studies (*13–15*) analyzing the static behavior by instrumenting prototype walls have indicated that the failure surface starts near the toe and propagates upward in a parabolic manner.

In this study, the internal failure surface is held constant at (45 + ϕ/2) for both the static and dynamic load conditions. It is possible that during dynamic loading, the location and shape of the failure surface changes from the location and parabolic shape observed in the static condition. Because of the dynamic interaction of the reinforcement with the soil, it is assumed that this change is small and that it does not materially affect the tie force evaluation.

Dynamic Tie Force Evaluation

The method used to derive the equation for the total tie force at any level of reinforcement is similar to the derivation of the static tie force by Binquet (*16*). The individual tie forces are calculated by considering the element bounded by line segments marked *ABCD* and enveloping the *i*th tie as shown in Figure 8. Also, shown in this figure is a freebody diagram of the element, where T represents the tie force assumed to be inclined at the same angle as the failure plane; R represents the resultant force on the element's failure plane inclined at an angle ϕ_1, the soil's internal friction angle; and C represents the force developed along the length of the element's failure plane due to cohesion of the backfill material. Cohesion is represented in the derivation of the total tie force because slightly cohesive soils are now used as backfill material in soil-reinforced walls (*17*). The assumption of the tie force's inclination is not critical to the method. Identical values of tie force are determined whether the force is assumed to act horizontally or inclined for $\phi_1 = 30$ degrees. Slightly different values are determined for a ϕ_1 other than 30 degrees.

In this study, the total force (dynamic plus static) is equal to the mass of the active wedge, as defined by the assumed failure plane, multiplied by the horizontal acceleration. This total force is proportionally distributed to each tie depending on the area of the active wedge enveloped by each tie. The numbered forces in Figure 8 represent the internal and external body forces. The vertical and horizontal components of all the forces shown in this figure are listed in Table 1.

By summing these forces, back substituting and solving for T, the tie force at the ith level shown in Equation 7 is found.

$$T_i = \frac{K_h MF - MV - CG}{G} \tag{7}$$

where

$$M = \gamma \Delta H^2 (\tan \theta)^{-1}$$
$$V = (i - N - 1/2)$$
$$G = 2\sin \theta$$
$$F = (i - 1/2)\tan \theta$$

Comparison With Rankine's Active Earth Pressure Coefficient

The tie force determined in the foregoing manner can be compared to the force determined using Rankine's active earth

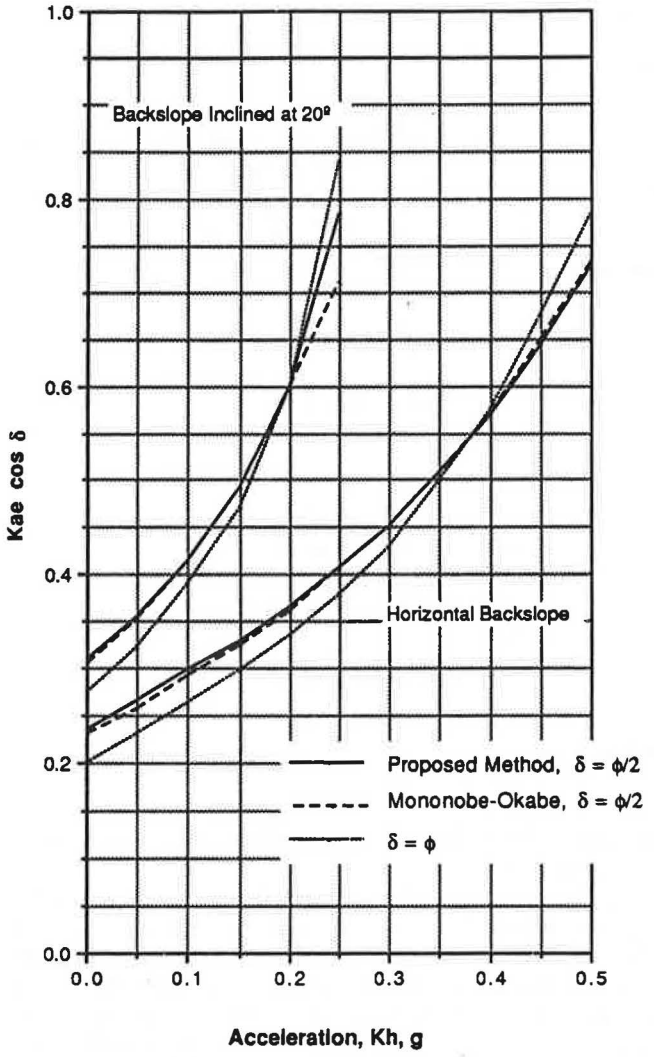

FIGURE 7 Comparison of dynamic earth pressure coefficients [after Seed and Whitman (*12*)].

pressure coefficient by setting the values of horizontal acceleration, K_h, and cohesion, C, equal to zero in Equation 7. When this is done, the absolute value of the tie force at any level is expressed as follows:

$$T_i = \frac{MV}{G} \tag{8}$$

Substituting the previously defined expressions for the values in Equation 8, the tie force is found to be:

$$T_i = Ka_1\gamma\,(N - i + 1/2)\Delta H^2 \tag{9}$$

where

$$Ka_1 = \frac{\sin(45 - \phi/_2)}{2\cos^2(45 - \phi/_2)}$$

When the tie force is calculated using Rankine's formula, the following relationship is derived:

$$T_i = Ka_2\,\gamma\,(N - i + 1/2)\Delta H^2 \tag{10}$$

where Ka_2 is equal to $\tan^2(45 - \phi/2)$, Rankine's active earth pressure coefficient.

The variation of the two coefficients, Ka_1 and Ka_2, is shown in Figure 9 as a function of friction angle. This figure shows that the methodology used results in slightly lower coefficients than the Rankine coefficients for friction angles less than 30 degrees, while the opposite is true for angles greater than 30 degrees.

Determination of Factors of Safety Against Yield and Pullout

Having determined the static and dynamic forces in the ties at all levels of embedment, the factors of safety against yield and pullout are determined next. The factor of safety against yield, FS_y, and against pullout, FS_p, are defined in the following equations:

$$FS_y = \frac{R_y}{T} \tag{11}$$

$$FS_p = \frac{R_p}{T} \tag{12}$$

where R_y and R_p are the respective resistances to yield and pullout of the ties per lineal foot of wall and T is the tie force per lineal foot. The results of laboratory and field pullout tests have commonly been reduced to a soil-reinforcement friction factor. In these tests, the friction factor, f, is determined by the following equation:

$$f = \frac{R_p}{P_v P_s EL} \tag{13}$$

where P_v is the vertical or overburden pressure, P_s is the perimeter of the reinforcing per lineal foot of wall, and EL is the embedment length behind the failure plane.

Values of friction factor as a function of overburden for different types of reinforcement and soil conditions are shown in Figure 10. The values were determined from both field and laboratory tests. Because the friction factor values have been shown to depend upon a number of factors like soil type, density, shear strength, and type of reinforcement, the pullout resistance for a given set of conditions would ideally be determined by field tests. In the absence of this type of data, the values shown in Figure 10 can be used.

In this study, Equation 13 is used to derive pullout resistance, R_p, at any level of reinforcement. In this equation, the values for P_v and EL, using the notation in Figure 8, are shown in Equations 14 and 15, respectively.

$$P_v = \gamma\Delta H(N - i + 1/2) \tag{14}$$

$$EL = OL - (\Delta H^* i/\tan\theta) \tag{15}$$

The soil-reinforcement friction factor, f, is modeled as a function of overburden pressure or level of reinforcement as shown in Equation 16.

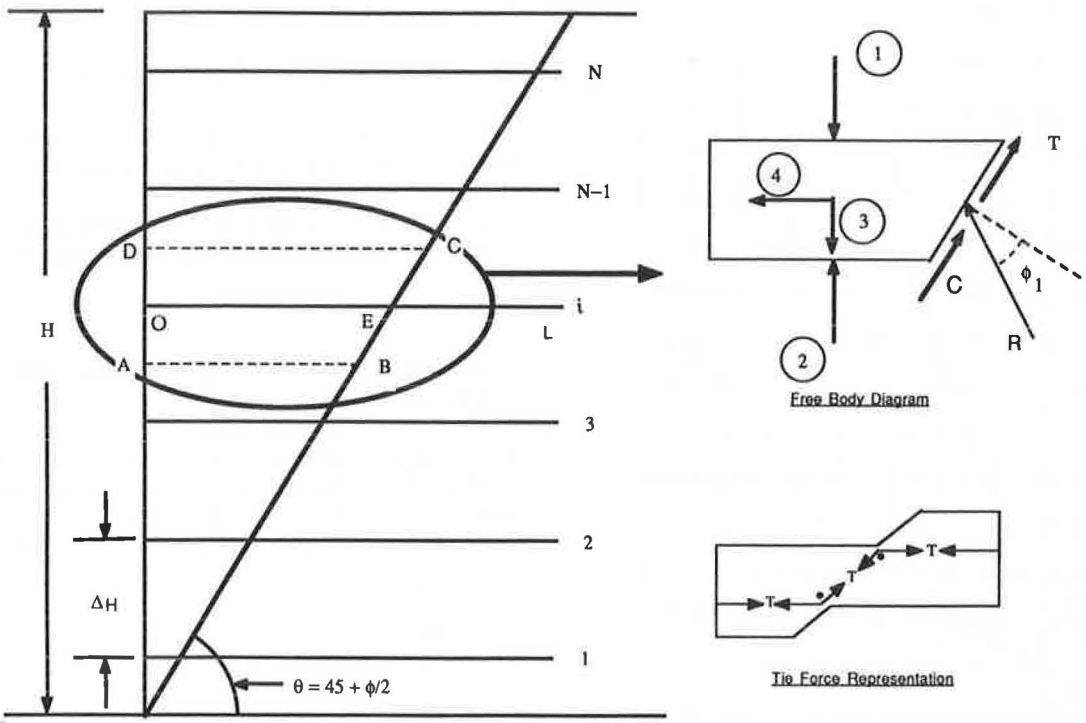

FIGURE 8 Representation of forces used to derive the total tie force.

TABLE 1 VERTICAL AND HORIZONTAL COMPONENTS OF FORCES SHOWN IN FIGURE 8

Force	Vertical	Horizontal
1	$-\gamma\Delta H^2(N-i)(i)\tan\theta^{-i}$	
2	$+\gamma\Delta H^2(N-i+1)(i-1)\tan\theta^{-1}$	
3	$-\gamma\Delta H^2(i-1/2)\tan\theta^{-1}$	
4		$-K_h\,\gamma\Delta H^2(i-1/2)\tan\theta^{-1}$
T	$+T_i\sin\theta$	$+T_i\cos\theta$
R	$+R_i\cos(\theta-\phi)$	$-R_i\sin(\theta-\phi)$
C	$+C\sin\theta$	$+C\cos\theta$

$$f_i = B_1 + B_2e^{-P_v} - B_3e^{-2P_v} \quad (16)$$

where B_1, B_2, and B_3 are constants obtained by solving three equations having friction values and corresponding overburden pressures in Kips obtained from either actual field/laboratory tests or the most applicable data shown in Figure 10.

Comparison With Previous Investigations

A computer program was written to perform the computations incorporating the proposed seismic design procedure (*18*). Data on the performance and behavior of a soil-reinforced wall during a seismic event is not known to exist. In view of this, the computer program was used to make predictions for tie forces and wall displacements for the 20-ft-high wall constructed and tested by explosives in the investigation by Richardson et al. (*4*).

In his investigation, Richardson placed explosives in front of the wall and 25 to 50 ft behind the wall at varying depths. The cumulative effect of a series of explosions in front of the wall resulted in a negligible total outward movement of 0.02 in., measured 6.3 ft below the top of the wall. In this series, the largest peak acceleration recorded at the base was 0.21 g, which was used as input to the computer program. The reinforcing used in construction of the wall consisted of longitudinal ties 80 mm wide and 3 mm thick. Because this type of reinforcing is similar to that used in establishing the curve for the smooth strips shown in Figure 10, a friction factor of 0.62 was input to determine the pullout resistance. Using the same soil and geometric properties of the wall, the model predicted no outward movement. The lowest factors of safety against yield, pullout, and sliding at the base were 5.9, 1.3, and 7.7, respectively.

The model predicted initiation of wall movements by sliding at the base at an acceleration of 0.6 g. At this level of acceleration, the factors of safety against pullout were less than unity for the upper four levels of reinforcement. The model predicted that the resistance to pullout at these levels would be exceeded at an acceleration of 0.43 g. The lowest factor of safety against yield was 5.5.

A series of explosives detonated behind the wall using larger amounts of dynamite produced base accelerations in excess of 0.8 g and resulted in a cumulative outward wall movement of 1.25 in. To quantify the displacements predicted by the model, it was noted that the explosive tests resulted in a single cycle of acceleration having a period generally less than 0.1 sec. Using this as a basis, a cumulative displacement of 0.62 in. was predicted.

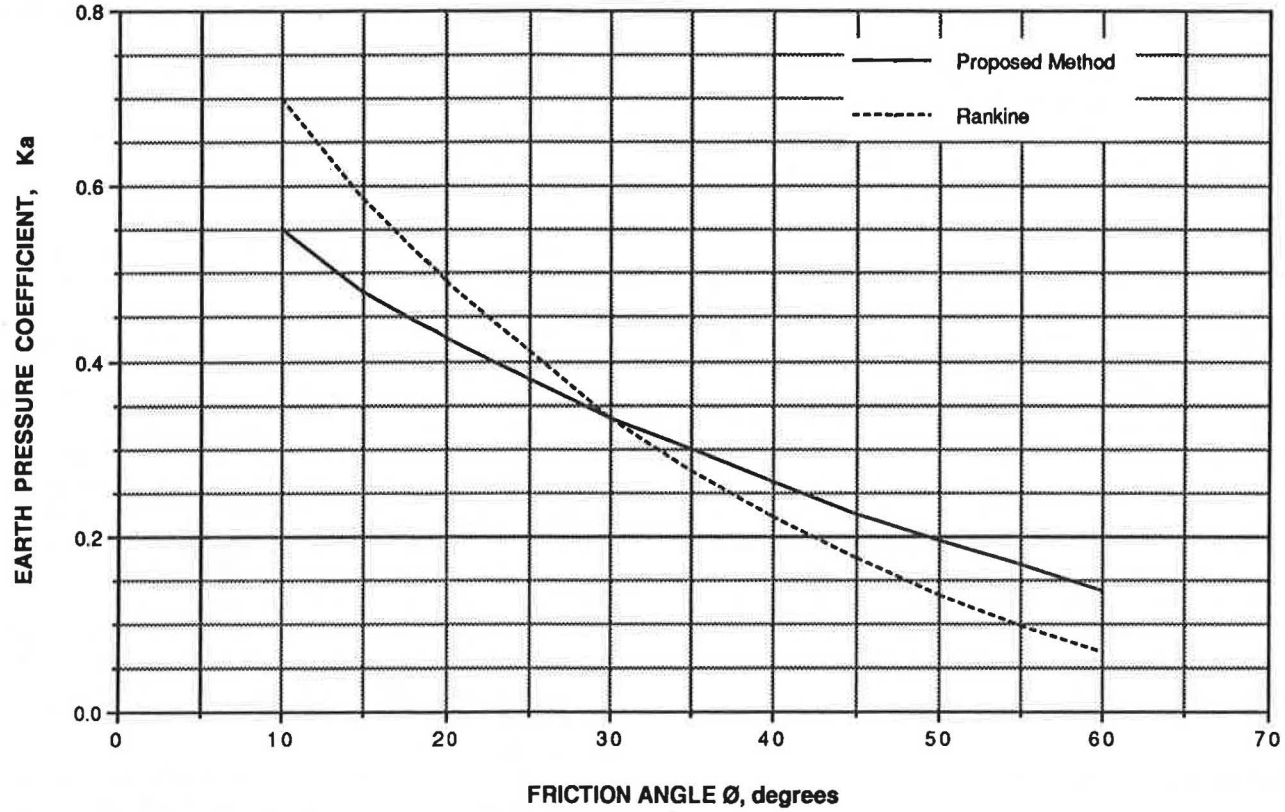

FIGURE 9 Comparison of Rankine active earth pressure coefficients.

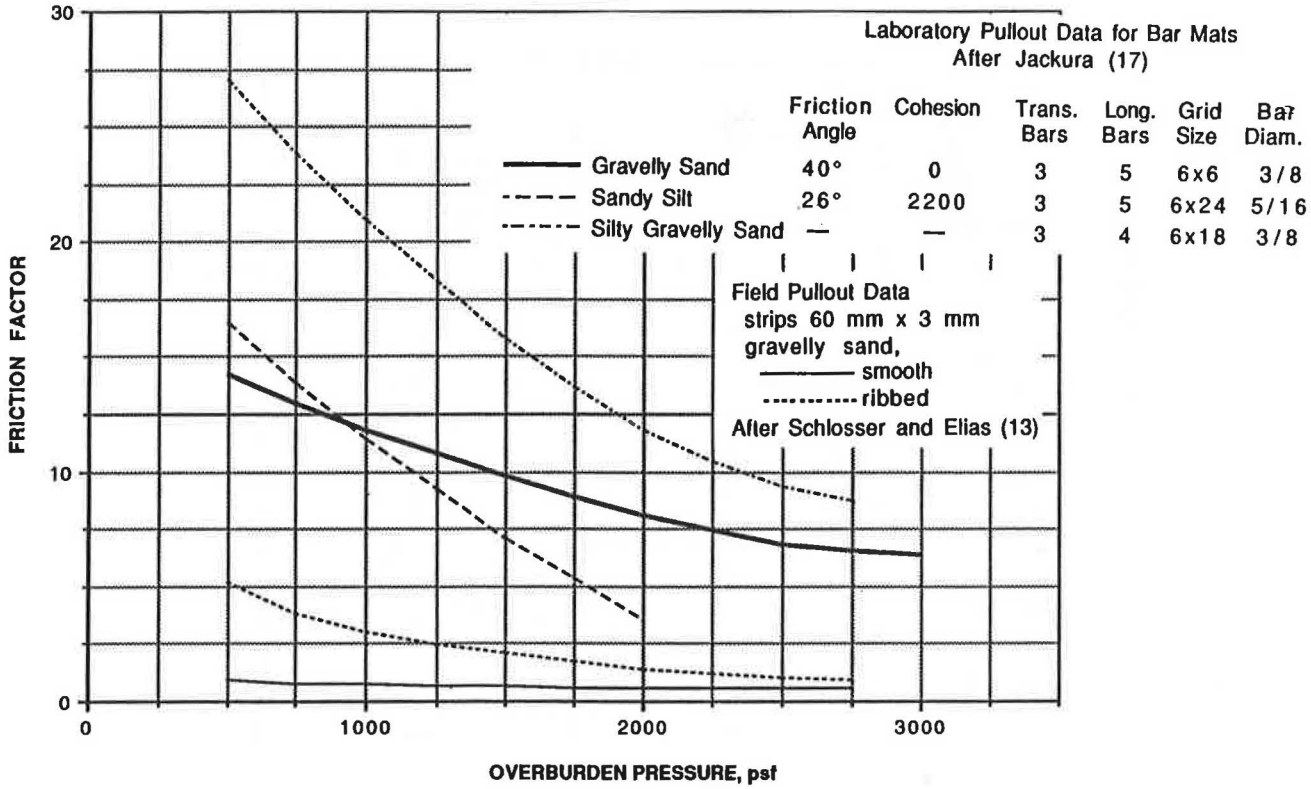

FIGURE 10 Variation of friction factor with overburden for different reinforcing elements and soil types.

Dynamic tie forces were also recorded and reported for an event that produced a peak acceleration of 0.08 g at the base. A comparison of these forces and the forces predicted by the model is shown in Figure 11. Also shown are the force levels predicted by the seismic design methodology based on the small-scale laboratory model studies. From this comparison it can be seen that the model predicts force levels approximately half-way between the explosive and laboratory model test results.

The observed cumulative displacement of the prototype wall is larger than what the model predicted. Because the primary effect of a blast is to move the wall outward, it is speculated that detonation of explosives behind the wall resulted in larger displacements than those caused by equivalent levels of acceleration applied at the base. This speculation is supported by the fact that the model overestimated the tie forces and correctly predicted the negligible observed displacement for the series of explosives detonated in front of the wall, while the model underestimated the displacements resulting from the explosive series placed behind the wall.

However, the model predicted relatively small displacements for events resulting in large levels of acceleration, while, similarly, small wall displacements were observed. This fact should not be overlooked.

PRACTICAL APPLICATION

The proposed seismic design was used to determine permanent displacements due to different earthquake loads for the 62-ft-high wall described in a companion paper by Jackura, elsewhere in this Record. The wall's site seismic parameters are controlled by the Maacama Fault. It is postulated, based on the fault's distance from the site, that the peak bedrock accelerations for the maximum credible (M7.5) and probable (M5.0) events are 0.7 g and 0.5 g, respectively.

The wall's overall dimensions and reinforcing type were entered into the computer program along with the applicable soil strengths for both the wall itself and the soil behind it. The upper curve shown in Figure 10 was selected to estimate the pullout resistance because the reinforcement is a bar-mat and the soil used to construct the wall approximates the soil for this curve.

For the external analysis, the variation of the factor of safety against sliding at the wall base with acceleration, as determined by the program, is shown in Figure 12. This figure shows the factor of safety dropping below unity at a level of acceleration greater than 0.49 g. No permanent displacement is predicted, therefore, for the postulated maximum probable seismic event producing 0.5 g at the site. For a peak acceleration of 0.7 g representing the maximum credible event, a permanent displacement of approximately 1 in. is predicted, which is considered well within tolerable limits.

The internal stability analysis is limited to considering peak accelerations up to and not exceeding 0.49 g, because sliding at the wall base is predicted to occur at that level. Therefore, any consideration of an acceleration time history for this analysis is capped at 0.49 g.

The variation of factors of safety against reinforcement pullout and yield with acceleration at three different levels of wall height is shown in Figure 13. This figure shows the factor of safety against pullout approaching unity for the top level of reinforcement while the factor of safety against yield approaches a value of 3 at the higher levels of acceleration for each of

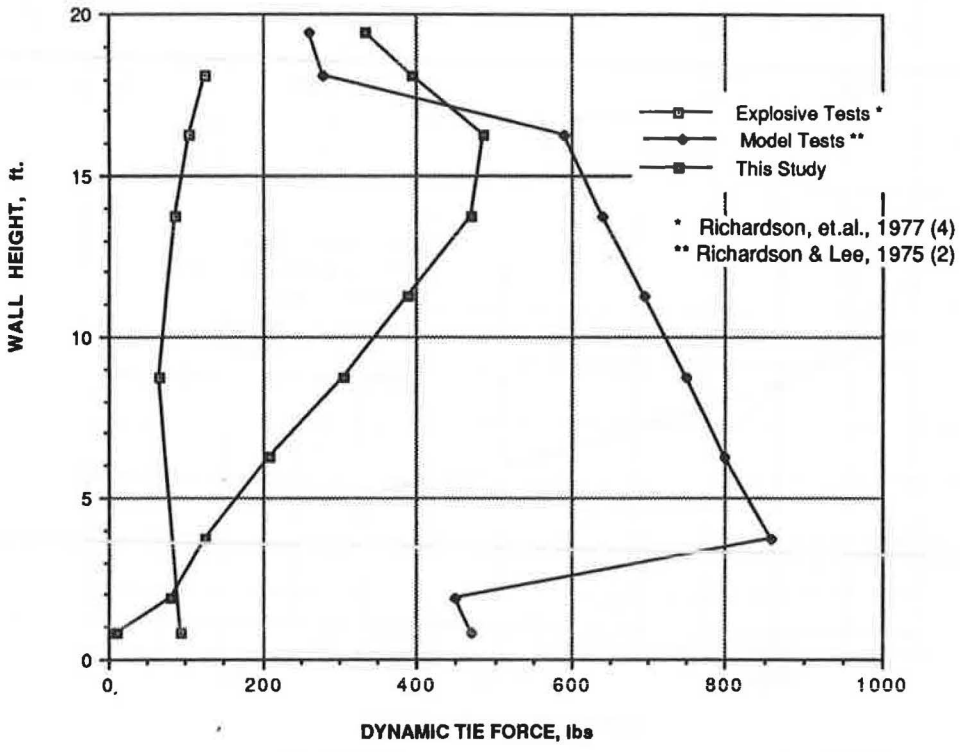

FIGURE 11 Comparison of dynamic tie forces, maximum base acceleration of 0.08 g [after Richardson et al. (*4*)].

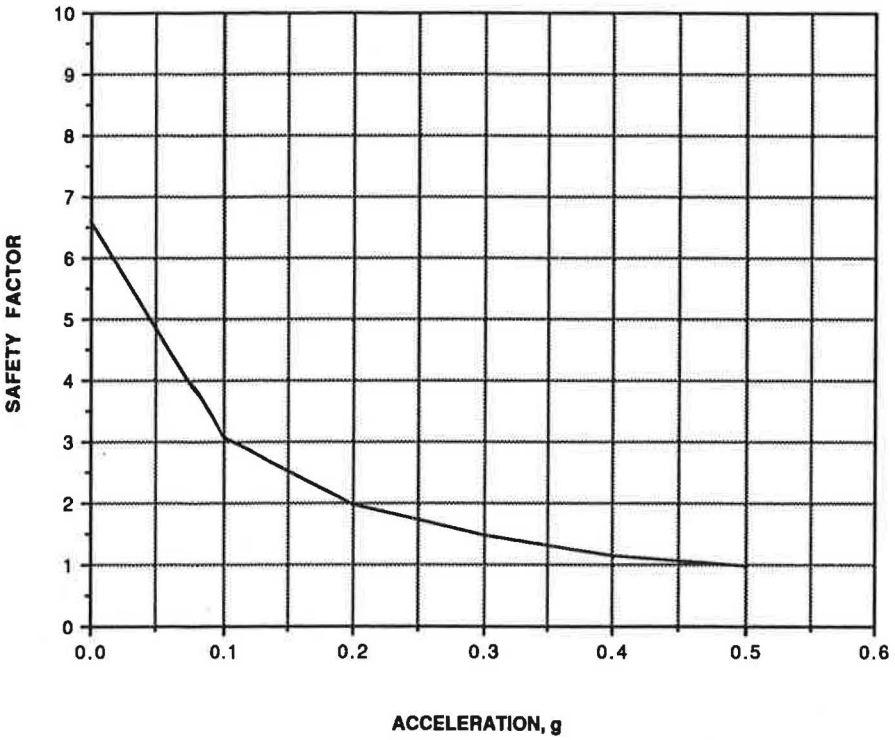

FIGURE 12 Influence of acceleration on the factor of safety against the wall sliding along its base.

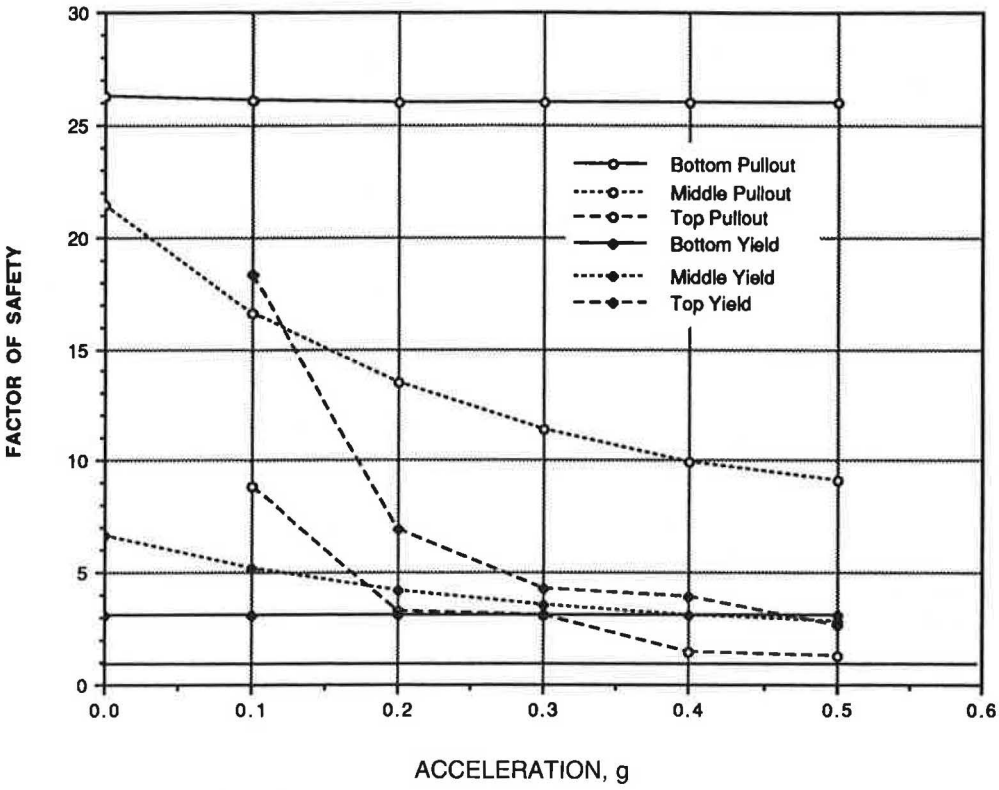

FIGURE 13 Variation of factor of safety against yield and pullout with acceleration for three levels of reinforcement.

the three levels of reinforcement. The factors of safety against yield shown in Figure 13 do not account for the effects of corrosion. Over the period of the wall's service life it is estimated that the reinforcement's cross-sectional area will be reduced by 50 percent due to corrosion. This would then reduce the yield factor of safety to 1.5 at 0.5 g, which is still sufficient to preclude the breaking or rupture of the reinforcement.

Based on the results of this analysis, the wall's design was considered adequate and the permanent displacements considered to be well within tolerable limits.

SUMMARY AND CONCLUSIONS

The proposed method described in this paper determines the factors of safety as a function of horizontally applied acceleration for both the external and internal stability of a soil-reinforced wall. The method was used to predict the performance of a 20-ft-high wall tested dynamically by explosive charges. The method's prediction compared favorably with the wall's observed behavior by predicting the level of acceleration at which movement would be initiated.

The method was then used to check the design and predict the performance of a 62-ft-high wall constructed in northern California. The design was found to be adequate and negligible permanent displacements were predicted for the postulated maximum credible seismic event.

It can be concluded that the method indicates initiation of sliding along a wall base at the higher levels of acceleration and that the upper layers of reinforcement are the most susceptible to pullout. This susceptibility to pullout can be mitigated by increasing the length of the reinforcement. Perhaps most importantly, the method indicates very small permanent displacement for Caltrans's current design of soil-reinforced walls under very severe seismic loading conditions.

Caltrans sponsors research at the University of California at Davis to verify and improve the method described. The research consists of testing model walls under both static and dynamic loads in the centrifuge. Preliminary results appear to validate the method and the assumptions used.

ACKNOWLEDGMENTS

A number of individuals on the Caltrans staff contributed to the development of the proposed methodology. Thang Le and Cuong Nguyen performed analyses and wrote portions of the computer program. Peter Dirrim performed analyses on the effect of capping acceleration time histories on their standardized displacements. Bruce Hartman combined the many elements of computer code and made the program user friendly. Their efforts, skills, and enthusiasm are acknowledged and greatly appreciated.

REFERENCES

1. H. Vidal. The Principle of Reinforced Earth. In *Highway Research Record 282*. HRB, National Research Council, Washington, D.C., 1969, pp 1–16.
2. G. N. Richardson and K. L. Lee. Seismic Design of Reinforced Earth Walls. *Journal of the Geotechnical Engineering Division*, ASCE Vol. 101, No. GT2, Feb. 1975, pp 167–188.
3. W. E. Wolfe, K. L. Lee, D. Rea, and A. M. Yourman. The Effect of Vertical Motion on the Seismic Stability of Reinforced Walls. *Proc., ASCE Symposium of Earth Reinforcement*, Pittsburgh, Pa. April 27, 1978.
4. G. N. Richardson, D. Feger, A. Fong, and K. L. Lee. Seismic Testing of Reinforced Earth Walls. *Journal of the Geotechnical Engineering Division*, ASCE Vol. 103, No. GT1, Jan. 1977, pp 1–17.
5. G. N. Richardson. Earthquake Resistant Reinforced Earth Walls. *Proc., ASCE Symposium on Earth Reinforcement*, Pittsburgh, Pa., April 17, 1978.
6. D. P. McKittrick and L. J. Wojciechowski. Design and Construction of Seismically Resistant Reinforced Earth Structures. *Proc., International Conference on Soil Reinforcement: Reinforced Earth and Other Techniques*. Vol. I, Paris, March 1979.
7. N. M. Newmark. Effects of Earthquakes on Dams and Embankments. *Geotechnique*, Vol. 15, No. 2, Jan. 1965.
8. R. Richards and D. G. Elms. Seismic Behavior of Gravity Retaining Walls. *Journal of the Geotechnical Engineering Division*, ASCE Vol. 105, No. GT4, April 1979, pp 449–464.
9. A. G. Franklin and F. K. Chang. Earthquake Resistance of Earth and Rockfill Dams. *Report 5: Permanent Displacements of Earth Embankments by Newmark Sliding Block Analysis*. Miscellaneous Paper S-71-17, Soils and Pavements Laboratory, U.S. Army Engineer Waterways Experiment Station, Vicksburg, Miss., Nov. 1977.
10. N. Mononobe and U. Matsuo. On the Determination of Earth Pressure During Earthquakes. *Proc., Ist World Conference on Earthquake Engineering*, Tokyo, Vol. 9, 1929.
11. S. Okabe. General Theory of Earth Pressure and Seismic Stability of Retaining Wall and Dam. *Journal of the Society of Civil Engineers*, Vol. 12, N1, 1920.
12. H. B. Seed and R. V. Whitman. Design of Earth Retaining Structures for Dynamic Loads. *Proc., ASCE Conference on Lateral Stresses, Cornell University*, Ithaca, N.Y., June 1970, pp 103–147.
13. F. Schlosser and V. Elias. Friction in Reinforced Earth. *Proc., ASCE Symposium on Earth Reinforcement*, Pittsburgh, Pa., April 27, 1978.
14. I. Juran, F. Schlosser, N. T. Long, and G. Legeay. Full Scale Experiment on a Reinforced Earth Bridge Abutment in Lille. *Proc., ASCE Symposium on Earth Reinforcement*, Pittsburgh, Pa., April 27, 1978.
15. U. Dash. Design and Field Testing of a Reinforced Earth Wall. *Proc., ASCE Symposium on Earth Reinforcement*. Pittsburgh, Pa., April 27, 1978.
16. J. Binquet. Analysis of Failure of Reinforced Earth Walls. *Proc., ASCE Symposium on Earth Reinforcement*, Pittsburgh, Pa., April 17, 1978.
17. K. Jackura. Results of Minor Research on Bar-Mat Pullout Tests. Office of Transportation Laboratory, California Department of Transportation, May 1984.
18. California Department of Transportation. DYNMSE–Computer Program to Evaluate the Dynamic Stability of MSE Walls. Office Report, July 1988.

Performance of a 62-Foot-High Soil-Reinforced Wall in California's North Coast Range

KENNETH A. JACKURA

California's Department of Transportation has constructed a realignment of a portion of Highway 101 near Cloverdale (about 85 miles north of San Francisco). To meet slope requirements and to prevent encroachment on a railroad, construction of four soil-reinforced retaining walls—62 ft, 48 ft, 40 ft, and 37 ft high—was required. The contractor chose a soil-reinforcement system consisting of a hexagonal concrete face panel and a galvanized steel bar-mat for reinforcement. Wall costs were determined by total area of the wall faces (61,100 ft²) and were bid at $30/ft². Wall construction was completed in 1988, and the entire project was completed in 1989.

In the summer of 1987, California Department of Transportation (Caltrans) began construction of a highway realignment project along Route 101 north of Cloverdale. The existing roadway at this location runs parallel along its east bank with the Russian River and the alignment has been moved to the west side of the river to remove it from an unstable slide area. The realignment has been designed with minimum 1.5:1 slopes in both the cuts and the fills to prevent localized sliding.

Highway design was complicated by the presence of a railroad track along the western bank of the river. At four locations, soil-reinforced walls were constructed to meet this restriction, as well to provide the required roadway width and to maintain the requirement that slopes not be steeper than 1.5:1 (Figure 1).

Foundation material varies from competent to fractured sandstone, beds of reddish mudstone, and hard resistant knobs of serpentine. Backfill for the walls was obtained within project limits, and consisted primarily of gravels with a clayey sand matrix.

The tallest of the walls is 62 ft high. It is instrumented with vertical and horizontal slope indicators, pressure cells, reference points, strain gauge bonded bar-mat reinforcements, and corrosion cells. After eight months of evaluation, instrumentation reveals stresses and movements well within acceptable limits.

DESIGN CONSIDERATIONS

Geology

The terrain of the proposed alignment is very steep. Project geology consists of relatively large "blocks" of sandstone, mudstone, greenstone, and chert, separated by shear zones of varying widths and intensity of deformation. A large serpentine body is present, separated from the other rock types by shear zones. All rocks are moderately to severely weathered and pervasively fractured.

Seismic Setting

The study area lies within a seismically active region. The closest known active faults are the Healdsburg Fault, approximately 3 miles southwest, and two recently discovered traces of the Maacama Fault zone, approximately 1 mile southeast.

The active San Andreas Fault is located 23 miles southwest of the project area and represents the major seismic hazard in northern California. Its maximum credible earthquake is a repeat of the 8.25 magnitude 1906 earthquake. The maximum accelerations in rock in the area resulting from earthquakes on these faults are shown in Table 1.

A full discussion of the earthquake design procedure used by Caltrans for design of soil-reinforced walls can be found in a companion paper in this Record by Vrymoed.

Design

Conventional retaining systems and viaducts are cost prohibitive because of the extreme heights of the roadway surfaces relative to the ground surfaces in the area combined with the variations in materials and conditions of the foundation.

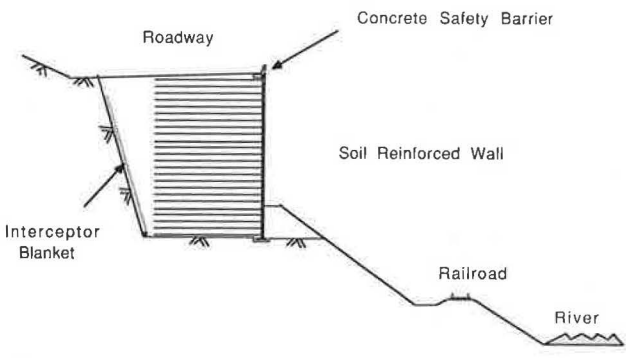

FIGURE 1 Typical section of soil-reinforced wall.

California Department of Transportation, Division of New Technology and Research, Office of Transportation Laboratory, 5900 Folsom Boulevard, Sacramento, Calif. 95819.

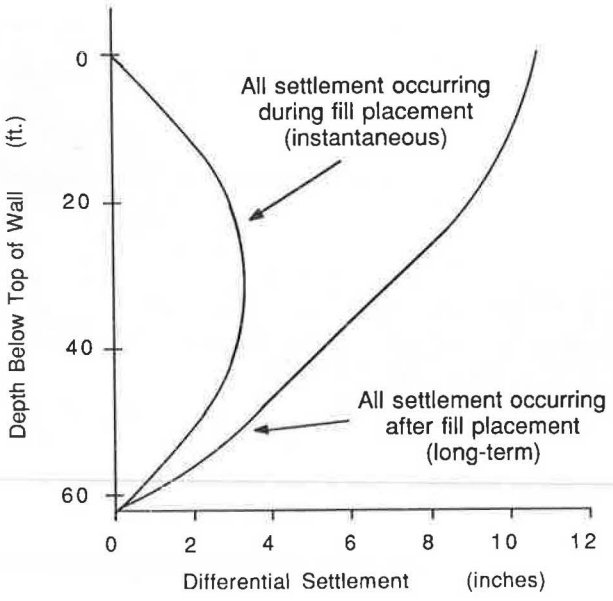

FIGURE 5 Maximum face to backfill differential settlement for two consolidation scenarios (wall height equal to 62 ft only).

High annual rainfall combined with subsurface water in many areas led to an extensive drainage design. Each gully or ravine filled during construction was drained by a pipe through the fill. As an additional precaution against water intrusion into the soil-reinforced walls, all walls have interceptor drains of crushed rock wrapped in filter fabric placed behind the reinforced zone (Figure 1). Intercepted groundwater is collected in perforated pipes at the bottom of the drains and carried to the face of the berm.

SAMPLING, TESTING, AND INSTRUMENTATION

Sampling and Testing

Compaction testing and backfill sampling were conducted daily to assure compliance with the project specifications. In situ testing was conducted using a nuclear gauge. Moisture and density curves for determination of the relative compaction were determined using California Test Method 216. Results showed that the backfill was in compliance with the specifications and indicated a lower bound average of 95 percent relative compaction.

At various heights of the walls, large samples (approximately 500 lbs) were taken for triaxial testing. Tests were conducted using 6-in. diameter triaxial test equipment with minus 1.5-in. material setup at the (field-measured) 95 percent relative compaction. Gradations were compensated to provide percentages of material passing the Number 4 sieve similar to the field-measured values. The tests were conducted in both saturated–undrained and saturated–quick-drained conditions. Tests considered most similar to long-term field behavior were the saturated–quick-drained tests. These tests were back-pressured to achieve full saturation, then the backpressure was relieved to atmospheric pressure prior to testing. Test results indicated an average angle of internal friction of 32 degrees with cohesion equal to 1,000 psf.

Instrumentation and Evaluation

Instrumentation was installed to provide for both construction and long-term monitoring of the walls. All four walls had slope indicators placed behind the face during construction. These slope indicators will provide information regarding movements of the reinforced mass.

Of the four walls, Wall 1035 is the highest (a 60-ft-long portion of the wall is 62 ft high and most of the wall is over 50 ft high) and the longest (687.5 ft). Most of the instrumentation of this project is concentrated in the tallest portion of this wall. Instrumentation of Wall 1035 is as shown in Figure 6 and is described below

Vertical Slope Indicators

Slope indicators for measuring lateral displacements were placed at the wall face at the same locations as the strain-gauged barmats. An additional indicator was placed in the 50-ft-high section of the wall face approximately 200 ft away.

Slope indicators were "brought up" with the backfill throughout the construction period. Readings were taken at approximately 10-ft increases in height of the wall. As can be seen in Figure 7, the measured outward movements were relatively small and in a manner consistent with normal lateral deflection associated with vertical settlement. Total movement of the wall face prior to the suspension of construction was approximately 1.3 in.

During the following eight months, approximately 0.4 in. of movement was recorded (Figure 8). (Movement in the

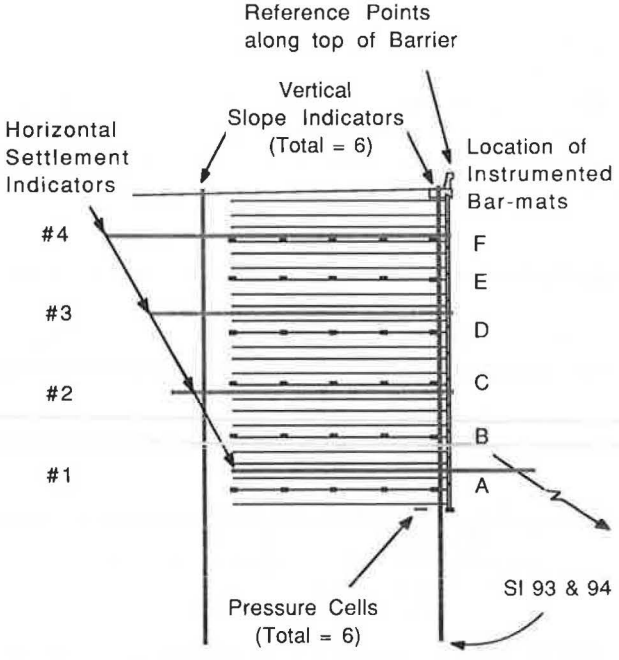

FIGURE 6 Instrumentation at Wall 1035.

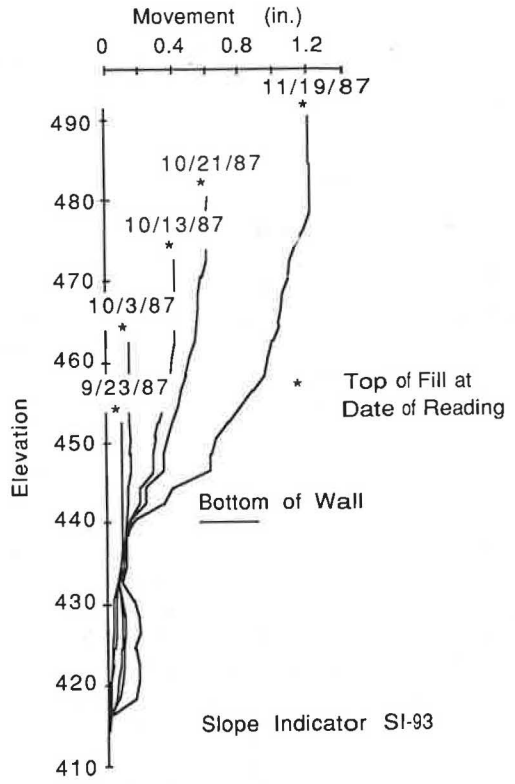

FIGURE 7 Outward movement at wall face during construction.

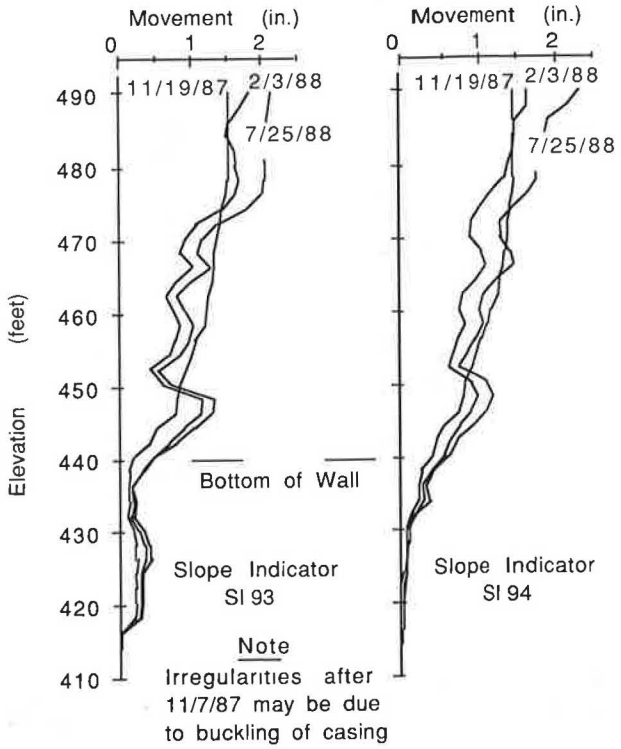

FIGURE 8 Outward movement at wall face after construction.

upper 5 ft to 7 ft is ignored). The rate of outward movement is decreasing, and the maximum long-term displacement is not expected to exceed 2 in. to 2.5 in. About 50 percent of all outward movement is estimated to be due to further construction loading processes, and the remainder due to differential toe-to-heel foundation settlement.

As evidenced in Figure 8, all slope indicators developed distortions during November and December 1987 (an initial rainy period). The slope indicators rest within the pea gravel zone immediately behind the wall face, and it is believed that down-drag forces induced by consolidation of the pea gravel caused buckling in the slope indicator casing, accounting for distorted displacements.

Three temporary slope indicators were placed in original ground some distance behind the reinforcement shortly after work was suspended for the winter. These indicators were used to compare face and original ground movement throughout the winter and were removed when construction in the area began in the spring. Displacements at these locations were negligible and are not shown.

Horizontal Settlement Indicators

Horizontal settlement indicators (HSIs) were placed at four levels in the wall—8, 23, 38, and 53 ft below the top of the wall (Figure 6). Differential settlement of the backfill relative to the face is readily apparent in the readings taken at various times throughout the winter and spring. Figure 9 shows the settlement for dates chosen to represent the suspension of construction (10/30/87), the end of winter (2/4/88), and the most recent reading (7/26/88).

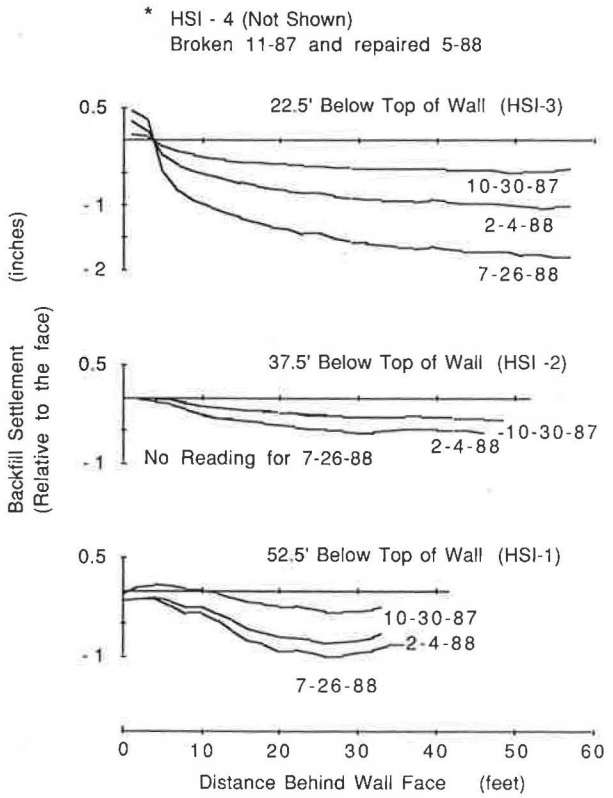

FIGURE 9 Backfill settlement with time.

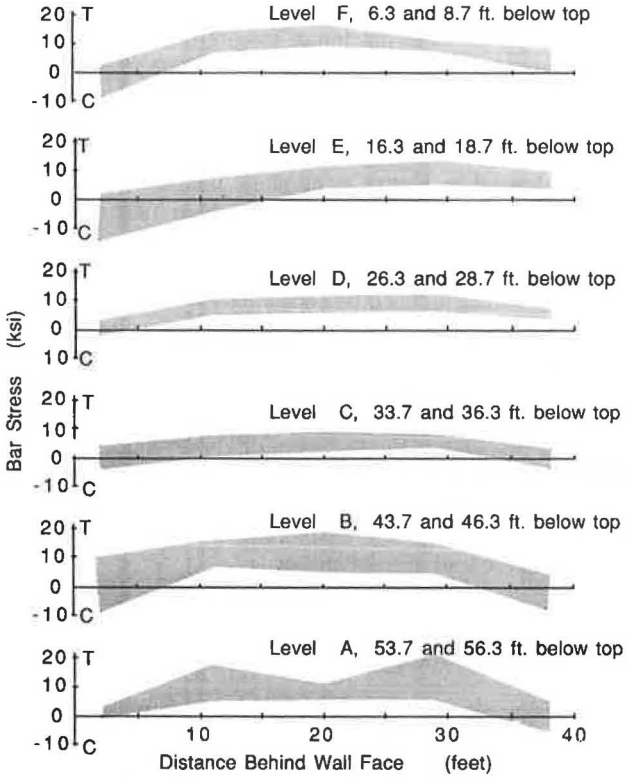

FIGURE 10 Range of stresses in bar-mats.

The upward movement near the face recorded by HSI-3 appears to be a result of an unsupported outer end of the indicator casing. The top indicator (HSI-4) is not shown because the casing was destroyed by the contractor in early winter and repaired in early summer.

Strain Gauges on the Reinforcement

At two places in the section of maximum height, six levels of bar-mats had strain gauges attached to their longitudinal wires. These mats were installed in the fill during the regular construction procedure. The strain gauges are located at 9-ft intervals along the length of the bar-mat (i.e., at 2, 11, 20, 29, and 38 ft). All gauges are attached in pairs, one on top and one on the bottom, to allow a full-bridge reading for strain. This configuration results in readings of strain due to axial stresses only.

In general, the strain gauges registered a consistent pattern of increasing stress. Figure 10 is a summary of the range of stresses for each level throughout the recording period. Note the relatively consistent stresses throughout the length of the bar-mats. This stress distribution is in contrast to the expected distribution—high stresses near a potential failure plane and diminishing with distance away from that area. The stress distribution will bear watching as roadway construction is completed and the structure goes through its first wet winter (California had a very dry winter during 1987–88).

Figure 11 shows the range of lateral earth pressures (as converted from bar-mat stresses) recorded at all locations.

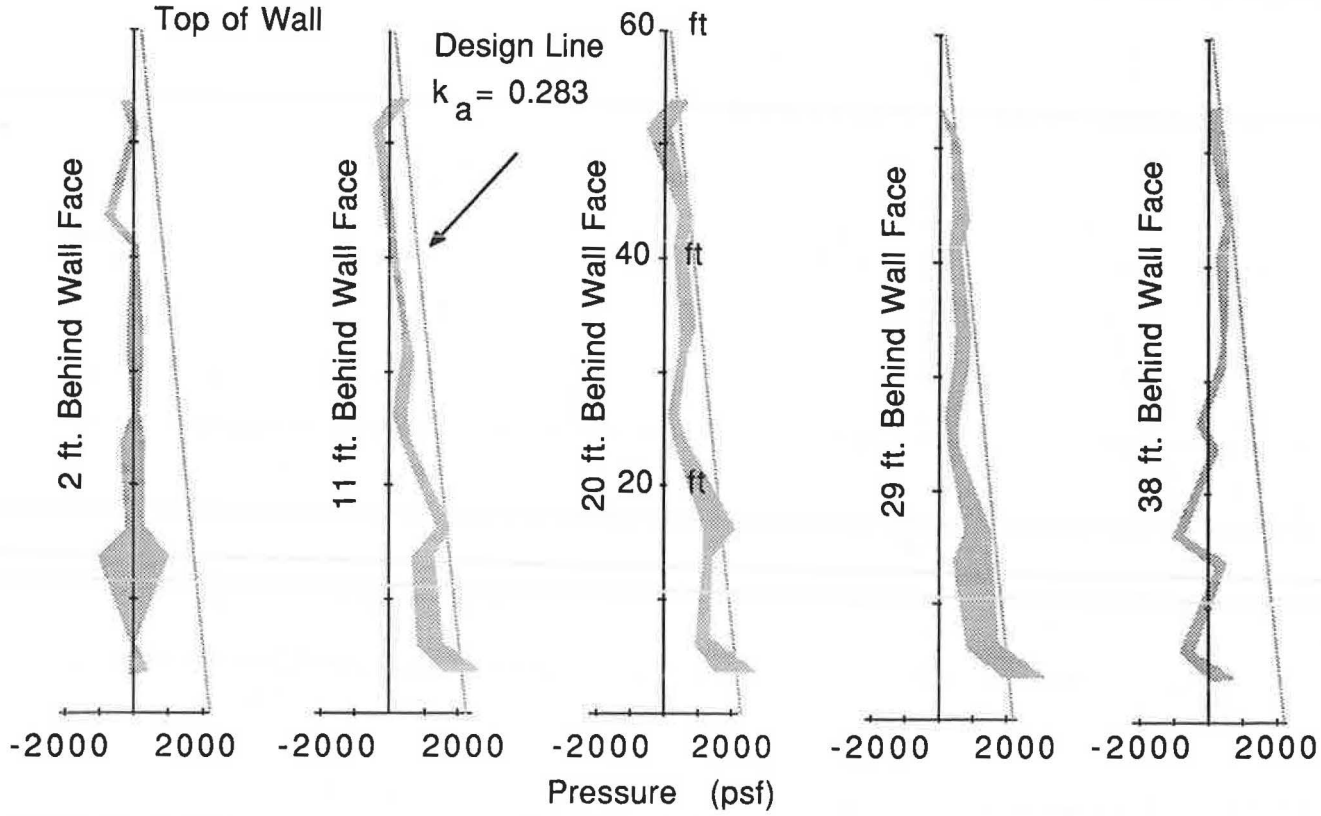

FIGURE 11 Range of lateral earth pressures as calculated from bar-mat stresses.

Most of these lateral earth pressures lie below design pressures (calculated using the design parameters of angle of internal friction equal to 34 degrees, no cohesion, and a soil unit weight of 120 pcf).

Pressure Cells

Six pressure cells were placed at the bottom of the wall approximately 4 ft behind the levelling pad. The cells were placed in holes excavated into the dense foundation material bedded on a 2-in. layer of sand, covered with 2 in. of sand, and the remainder of the hole was filled to grade with well-compacted native material.

With the exception of the earliest readings, the pressure cells have been registering significantly lower toe pressures than the height of fill suggests (data not shown). Performance of the pressure cells is not suspected as the cause for the low readings. A possible explanation for the low pressures is that soil stiffness within the excavated area is not as high as the surrounding in situ conditions. Thus, some soil arching may have occurred. Coupling this with probable bridging effects due to the bar-mat reinforcement located several feet above the cells, it is possible that the full overburden loading is not being transmitted to the cells.

Corrosion Monitoring System

During construction, a corrosion monitoring system using reference electrodes of bare steel, galvanized steel, zinc, and copper was placed at various levels in the highest part of the wall. These cells are being used for a separate study initiated with the objective of predicting corrosion rates by using external voltage.

In addition, pieces of the same steel as that used for the bar-mat reinforcement were placed at various depths and locations throughout the wall length. These bars will be removed at 5-yr intervals to monitor the corrosion rates of the bar-mat reinforcement. They are part of an ongoing study by Caltrans regarding the corrosion rates of steel-reinforcing elements of all soil-reinforcement systems.

SUMMARY AND CONCLUSIONS

In summary, the soil-reinforced walls discussed in this paper were reasonably easy to construct, represented a cost savings, and have performed well for the first year.

Instrumentation information in the 62-ft-high portion of the largest wall revealed no unanticipated amounts of deflection or bar-mat stresses either during construction or for the 8-month period following. Differential settlement between the wall face and the backfill, a particular area of concern, is minimal and not nearly as high as expected. Maximum backfill settlement is less than 2 in., also considerably less than anticipated. The small settlements are undoubtedly due to the high compaction achieved during backfill placement and the lateral restraint within the reinforced soil block offered by the bar-mat reinforcement.

Pea gravel placed directly behind the face panels, for approximately 3 ft, greatly facilitated construction by eliminating hand compaction and by limiting the amounts of face panel movement due to the compaction process.

The construction of these tall walls in difficult terrain indicates that their viability may exceed that of more conventional structures. The innovative corrosion instrumentation, along with the stress and deformation instrumentation, will provide a degree of long-term evaluation that will benefit future studies on these "passive" soil-reinforced retaining structures.